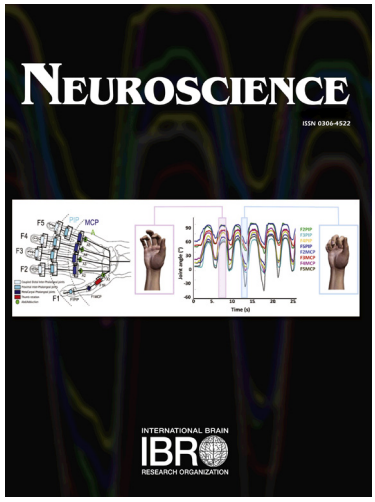

The $GABA_A$ α5-selective modulator, RO4938581, rescues protein anomalies in the Ts65Dn mouse model of Down syndrome

A. Block, Md.M. Ahmed, N. Rueda, M-.C. Hernandez, C. Martinez-Cué, K.J. Gardiner

PII: S0306-4522(17)30928-4
DOI: https://doi.org/10.1016/j.neuroscience.2017.12.038
Reference: NSC 18208

To appear in: *Neuroscience*

Received Date: 8 August 2017
Accepted Date: 21 December 2017

Please cite this article as: A. Block, Md.M. Ahmed, N. Rueda, M-.C. Hernandez, C. Martinez-Cué, K.J. Gardiner, The $GABA_A$ α5-selective modulator, RO4938581, rescues protein anomalies in the Ts65Dn mouse model of Down syndrome, *Neuroscience* (2017), doi: https://doi.org/10.1016/j.neuroscience.2017.12.038

The $GABA_A\alpha5$-selective modulator, RO4938581, rescues protein anomalies in the Ts65Dn mouse model of Down syndrome

A Block[a], MdM Ahmed[a], N Rueda[b], M-C Hernandez[c], C Martinez-Cué[b], KJ Gardiner[a,d]*

[a]Linda Crnic Institute for Down Syndrome, University of Colorado Denver School of Medicine; [b] Department of Physiology and Pharmacology, Faculty of Medicine, University of Cantabria, Santander, Spain; [c] Pharma Research and Early Development, F. Hoffmann-La Roche Ltd., Basel, Switzerland; [d]Department of Pediatrics, Human Medical Genetics and Genomics, and Neuroscience Programs, University of Colorado Denver School of Medicine, 12700 E 19th Avenue, Mail Stop 8608, Aurora, Colorado 80045, USA.

*corresponding author
katheleen.gardiner@ucdenver.edu
303-724-0572

Abbreviations

AD, Alzheimer's disease; AMPA, α-amino-3-hydroxy-5-methyl-4-isoxazolepropionic acid; BDNF, brain derived neurotrophic factor; CFC, context fear conditioning; CS, context-shock; DS, Down syndrome; FDR, false discovery rate; FvN, failed vs. normal learning; $GABA_A$, gamma-aminobutyric acid; GAD2, glutamic acid decarboxylase-2; Hsa21, human chromosome 21; ID, intellectual disability; IEF, iso-electric focusing; IEG, immediate early gene; KEGG, Kyoto Encyclopedia of Genes and Genomes; LTD, long term depression; LM, learning/memory; LTP, long term potentiation; MAPK, Mitogen-Activated Protein Kinase; Mmu16, mouse chromosome 16; MTOR, Mammalian Target of Rapamycin; MWM, Morris Water Maze; NAM, negative allosteric modulator; NMDA, N-methyl-d-aspartate; NRvN, normal learning + RO4038581 vs normal learning + vehicle; RvF, partially rescued vs. failed learning; SC, shock-context.

Abstract

Down syndrome (DS), trisomy of human chromosome 21, is the most common genetic cause of intellectual disability (ID). There are no treatments for the cognitive deficits. The Ts65Dn is a partial trisomy mouse model of DS that shows learning and memory (LM) impairments and other abnormalities relevant to those seen in DS. Many drugs and small molecules have been shown to rescue the LM deficits, but little is known about the associated molecular responses. Here, patterns of protein expression are described in hippocampus of Ts65Dn and euploid littermate controls exposed to a battery of LM and behavior tests with and without chronic treatment with the $GABA_A$ receptor α5 subunit-selective negative allosteric modulator, RO4938581, that rescued LM deficits. Levels of 91 proteins/protein modifications, selected for relevance to LM and synaptic plasticity, were measured: 44 of 52 abnormalities present in vehicle-treated Ts65Dn were corrected by RO4938581. Superimposing protein data onto the molecular pathway defining long term potentiation (LTP) shows that profiles are consistent with both abnormal LTP in vehicle-treated Ts65Dn and its observed rescue by RO4938581. Lastly, comparing these results with those from Ts65Dn treated, using a different protocol, with the NMDA receptor antagonist, memantine, that also rescues LM impairments, identifies common and divergent responses to the two drugs. Expansion of this approach to include additional drugs and DS models would aid in determining critical protein abnormalities and in identifying cocktails of drugs and/or new drug targets that would be effective in clinical trials for ID in DS.

Key words

Hippocampus, cognition, memantine, clinical trials, protein profiling, reverse phase protein arrays

Introduction

Down syndrome (DS), also known as trisomy 21, is caused by an extra copy of all or, rarely, part of human chromosome 21 (Hsa21). The phenotype of DS is variable among individuals in the extent of organ systems affected and in severity (reviewed in Karmaloff-Smith et al.. 2016), but common to all individuals is some level of intellectual disability (ID) (Chapman and Hesketh 2000; Silverman 2007). With a worldwide incidence of approximately one in 700-1000 live births, DS is the most common genetic cause of ID (CDC 2006; Irving et al.. 2008; Parker et al. 2010). Because the life expectancy is now ~60 years, people with DS represent an increasingly significant proportion of the population (Irving et al. 2008; Glasson et al. 2002; Bittles and Glasson 2004; Bittles et al. 2007; Kucik et al. 2013; Glasson et al. 2016; de Graaf et al. 2016). There are, however, no pharmacological treatments for the cognitive deficits.

DS is not simple to model in mouse because orthologs of Hsa21 protein coding genes map to three mouse chromosomes, Mmu16, 17 and 10 (Davisson et al. 1990). Many mouse models have been constructed, all partial trisomics (reviewed in Gupta et al. 2016; Choong et al. 2015; Rueda et al. 2012; Herault et al. 2012; Roubertoux and Carlier 2010). Of these, the oldest and most popular is the Ts65Dn that is trisomic for most of the Mmu16 orthologous region, encompassing 90 of the ~160 Hsa21 non-keratin associated protein orthologs (Davisson et al. 1990; Davisson et al. 1993; Reeves et al. 1995; Gupta et al. 2016). The Ts65Dn has been extensively analyzed in its >25 year history and has been shown to manifest many features similar to those seen in people with DS, including reduced sizes of the hippocampus and cerebellum, abnormal neuronal densities and morphologies, and impaired learning and memory (LM) in tasks requiring a functional hippocampus (reviewed in Rueda et al. 2012; Roubertoux and Carlier 2010). Other phenotypic features of the Ts65Dn include impaired adult neurogenesis and abnormalities in electrophysiological properties of long term potentiation (LTP) and long term depression (LTD) (Holtzman et al. 1996; Siarey et al. 1997; Kleschevnikov et al. 2004).

The Ts65Dn is currently the model used in preclinical evaluations of pharmacotherapies for cognition in DS. Over that last several years, >20 drugs, small molecules and nutritional supplements have been shown to successfully rescue performance of the Ts65Dn in one or more LM tasks (reviewed in Gardiner 2009; Das and Reeves 2011; Gardiner 2014). These drugs are diverse in their targets and mechanisms of action. With one exception, they have not been chosen because they target an Hsa21-encoded gene product, but rather because they target a downstream

cellular or molecular abnormality observed or predicted in the Ts65Dn or the DS brain. Examples of such abnormalities, and the drugs that rescue them, include serotonin levels and impaired adult neurogenesis rescued by fluoxetine (Clark et al. 2006); repressed LTP associated with increased gamma-aminobutyric acid-A-($GABA_{A)}$-mediated inhibition rescued by $GABA_A$ receptor antagonists, pentylenetetrazole and picrotoxin (Fernandez et al. 2007) and α5-$GABA_A$ negative allosteric modulators (NAMs) RO4938581 and α5IA (Martínez-Cué et al. 2013, Braudeau et al.. 2011a); increased N-methyl-D-aspartate (NMDA) receptor activation targeted by memantine (Costa et al. 2008); oxidative stress targeted by vitamin E (Busciglio et al. 1995; Lockrow et al. 2009; Coskun et al. 2012; Shichiri et al. 2011); and inflammation targeted by minocycline (Hunter et al. 2004). Most often, outcome measures for preclinical evaluations in the Ts65Dn have involved performance in one or more LM tasks, sometimes measurement of LTP and neurogenesis, but rarely molecular assessments. Consequently, little is known about the molecular responses that underlie improved LM and, importantly, how diverse drugs can result in the common outcome of successful LM.

Previously, we reported protein expression in the Ts65Dn after treatment with memantine, with and without exposure to LM in context fear conditioning (CFC) (Ahmed et al. 2014, 2015). Responses were complex, with significant involvement of mitogen-activated-protein-kinase (MAPK) and mechanistic-target-of-rapamycin (MTOR) pathways, as well as ionotropic glutamate receptor subunits and interacting proteins. To distinguish abnormalities that contribute to LM impairment from those that compensate for the initial trisomy-induced abnormalities, and to identify drug responses critical to rescue of LM impairment, it is necessary to examine effects of additional drugs.

Increased $GABA_A$-mediated inhibition has been proposed to be a crucial mechanism contributing to the LM alterations found in the Ts65Dn mouse. This has motivated the testing of several compounds for reduction of inhibition (Fernandez et al. 2007; Braudeau et al. 2011 a, b; Martinez-Cué et al. 2013). RO4938581 (3-bromo-10-(difluoromethyl)-9H-benzo[f]imidazo[1,5-a][1,2,4]triazolo[1,5-d][1,4]diazepine) is a $GABA_A$ receptor NAM, with dual binding and functional affinity specific for $GABA_A$ receptors containing the α5 subunit (Ballard et al. 2009). Chronic oral administration of RO4938581 to Ts65Dn mice has been shown to improve LM and to rescue LTP and neurogenesis, without the side effects, such as anxiety and convulsions, seen with non-selective $GABA_A$ receptor modulators (Martinez-Cué et al. 2013). No Hsa21 encoded

genes are known to affect $GABA_A$ receptor function or signaling, and the molecular mechanisms underlying the functional and morphological rescue of Ts65Dn phenotypes by this NAM have not been investigated. Here, we report analysis of Ts65Dn hippocampal protein expression after treatment with the $GABA_A\alpha5$ NAM, RO4938581.

Experimental procedures

Mice

Brain tissue was obtained from two sets of male mice. Set 1 included 4-5 mice per genotype-treatment group (Ts65Dn and euploid controls, treated with vehicle and drug) from those previously reported by Martínez-Cué et al. 2013. Set 2 included an additional 5-7 mice per genotype-treatment group subjected to a similar protocol as Set 1. In both Set 1 and Set 2, male Ts65Dn and littermate controls, at 3-4 months of age, were given either chocolate milk (Puleva, Spain) alone (vehicle) or chocolate milk containing the $GABA_A\alpha5$ NAM, RO4938581 (Hoffman-La Roche, Basel, Switzerland; 20 mg/kg). Under the conditions used here, RO4938581 crosses the blood-brain barrier, based on our observation that, in both euploid controls and Ts65Dn, 20 mg/kg RO4938581 decreased specific binding of [^{3}H]RO0154513 (an analog which has high affinity for the $GABA_A\alpha5$ subunit) in hippocampus by 68% and 72%, respectively (Martinez-Cué et al 2013). The dose of 20 mg/kg RO4938581 in 150 µl was chosen because it led to plasma concentrations that correlated with 50– 70% $GABA_A$ α5 receptor occupancy (Martinez-Cué et al. 2013).

Prior to the start of experiments, Ts65Dn and euploid control mice were conditioned to drink chocolate milk: each day, for one week, mice were individually placed in a clean standard cage containing a small Petrie dish with 150 µl of chocolate milk. After drinking the milk, mice were returned to their home cage; all mice drank all the chocolate milk within 5 minutes. During the next 6 weeks, every day at 10:00 AM, mice were again placed into a clean cage now with either milk alone or milk plus RO4938581 and returned to their home cage after drinking. During the subsequent 6 weeks, the drug/milk protocol continued while mice were exposed to behavioral assessments. All mice consistently consumed the entire chocolate milk–drug mixture.

Behavioral assessments

The battery of behavioral and LM tasks, included in order: actimetry, reflex test battery, rotarod, open field, elevated plus maze, hole board, and the Morris water maze (MWM) as described in detail in Martínez-Cué et al. (2013). Briefly, the spontaneous activity test measured the animal's locomotor activity during a complete light/dark cycle of 24 h. In this test, the Acti-System II (Panlab) apparatus measures the changes in a magnetic field produced by the animal's movement. In the visual placing reflex test, cerebellar and vestibular functions were evaluated. To evaluate auditory sensitivity, the startle response to a sudden auditory stimulus was measured. To evaluate equilibrium, four 20 s trials of balance were performed on a 40 cm high, 50 cm long horizontal rod. Trials 1 and 2 were performed on a 9 mm wide flat wooden rod; trials 3 and 4 used a 1 cm diameter cylindrical aluminum rod. Prehensile reflex (three 5 s trials) was measured as the ability of the animal to remain suspended by the forepaws by grasping an elevated 2 mm diameter horizontal wire. Motor coordination was evaluated on a 37 cm long, 3 cm diameter plastic rod that rotated at different speeds (Ugo Basile). In a single session, four trials with a maximum duration of 60 s each were performed. In the first three sessions, the rod rotated at constant speeds of 5, 25, and 50 rpm, respectively. In the last trial, the rod rotated progressively faster. The length of time that each animal stayed on the rotarod during the acceleration cycle was recorded. The modified version of the Morris Water Maze, used to evaluate spatial learning and memory, was described in Martínez-Cué et al. (2013). Briefly, mice were exposed to 16 consecutive daily sessions: 12 acquisition sessions (platform submerged 1 cm), followed by a probe trial and four cued sessions (platform visible). During the first eight sessions, the platform quadrant location was changed every day to assess spatial working memory. In sessions 9–12, the platform was placed in the SW quadrant (standard protocol) to assess spatial learning. Set 1 mice were administered the drug or vehicle 60 minutes before the start of each session; 24 hours after session 12, mice were exposed to a probe test. Set 2 mice received the drug or vehicle 60 minutes before each of sessions 1-8, but 60 minutes after each of sessions 9-12; Set 2 mice were not subjected to a probe trial. Set 2 mice were studied after publication of Set 1 mice (Martinez-Cué et al. (2013). The change in timing of drug treatment in sessions 9-12 was used to determine if the LM improvement seen in the MWM persisted when the drug was no longer present in the receptor (RO4938581 has an elimination half-life of one hour). However, because proteomic analysis was to be carried out on both sets of mice, it was important that all mice receive the same daily dose of drug/milk. Therefore, to be consistent with Set 1 mice in daily dose of

milk/drug, Set 2 mice instead received the drug/milk 60 minutes after MWM exposure. There were no statistically significant differences between Set 1and Set 2 mice in performance of any task. MWM performance for the two sets of mice are shown in Figure 1(complete data available from the authors).

After completion of testing, both Set 1 and Set 2 mice were sacrificed by cervical dislocation without anesthetic 60 minutes after treatment with drug or vehicle; the hippocampus was rapidly dissected out, flash frozen in liquid nitrogen, and shipped on dry ice to the University of Colorado Denver. Information for each mouse on age and littermates is provided in Appendix A (available from the authors). For analysis of protein expression, data from mice from corresponding genotype/treatment groups from Set 1 and Set 2 were pooled, resulting in 10-12 individuals per group. Because there were slight differences between Set 1 and Set 2 mice in the timing of drug administration during the last sessions of the MWM, pooling was used to identify protein responses that are common to both Set 1 and Set 2 mice. Mice used in protein expression data obtained from Ts65Dn and euploid controls exposed to context fear conditioning with and without treatment with the NMDAR open channel blocker, memantine, have been described (Ahmed et al. 2014, 2015).

Protein lysates and reverse phase protein arrays

Procedures for preparation of hippocampal lysates and printing and screening of reverse phase protein arrays (RPPA) were as described (Ahmed et al. 2011, 2012, 2013). Briefly, to optimally preserve protein profiles, tissues were removed from the freezer and, without thawing, heat stabilized in the Stabilizor T1 (Denator, AB), as previously described (Ahmed and Gardiner 2011; Ahmed et al 2012). Protein lysates from individual hippocampal samples were prepared by standard protocols in isoelectric focusing (IEF) buffer [8 M urea, 4% 3-[(3-cholamidopropyl) dimethylammonio]-1-propanesulfonate (CHAPS), 50 mM Tris]. Protein concentrations for all samples, measured by the 660 nM Protein Assay kit (Pierce), were within the range of 9-11 mg/ml. Samples were printed, in triplicates of a five point dilution series, onto nitrocellulose-coated glass slides (Grace Bio-Laboratories, Inc., Bend, OR) using an Aushon BioSystems 2470 Arrayer (Aushon BioSystems, Billerica, MA). The arrays were produced in two print runs and slides were stored at 4^{o}C until use.

For antibody screening of arrays, slides were incubated in blocking solution, followed by primary and secondary antibodies using protocols similar to those for Western blots as described in Ahmed et al 2012. Bound primary antibodies were detected using Alexa Fluor 555 goat anti-mouse or anti-rabbit or rabbit anti-goat (Invitrogen, Camarillo, CA, USA). To control for variation in protein concentration between spots, total protein in each spot was assessed by staining three non-sequential slides from each print run with the general protein stain SyproRuby following the manufacturer's directions. For use in all analyses, antibody signal was normalized to the corresponding SyproRuby signal. Details of quantification, review of data quality and reproducibility were as described previously (Ahmed et al 2012; see also http://downsyndrome.ucdenver.edu/iddrc/rppaware/home.htm). RPPA is a high throughput dot blot procedure. It has been extensively validated for accuracy and reproducibility in our own work (Ahmed et al 2012) and in that of others (Espina et al 2007; Pierobon et al 2011). Indeed, its reliability has supported its use in clinical trials for cancer prediction and prognosis (reviewed in Pierobon et al 2015). Small sample volumes precluded use of Western blots. A list of all antibodies and files containing SyproRuby and all antibody raw signal intensities are provided in Appendix B (available from the authors).

Statistics

Each genotype-treatment group was composed of a total of 10-12 mice, 4-7 each from Set 1 and Set 2. Data from individual mice in Set 1 and Set 2 in the corresponding groups were pooled, (i) because behavioral performances did not differ significantly between Set 1 and Set 2 corresponding genotype/treatment groups and (ii) in order to identify protein responses that were common to the corresponding groups in the two sets. Each SyproRuby normalized protein value was included in the statistical analysis if the level was within +/-10% of the mean of the 15 spots for that sample. Samples with fewer than 7 normalized protein values within 10% of the mean for a specific antibody were eliminated from calculations for that antibody; fewer than 5% of sample measurements were removed. Mean differences between genotypes of each treatment (trisomy vs. control, reported as % of control) and between treatments (drug vs. vehicle) for each genotype were assessed using a hierarchical three-level mixed effects model (3LME). 3LME is commonly used in cases where multiple measurements are made on the same subject which can give rise to erroneous significance in relationships between groups

(www.stat.cmu.edu/~hseltman/309/Book/chapter15.pdf). 3LME is appropriate here because for each protein, each sample was printed in three replicates of a 5 point dilution series, i.e. 15 measurements per sample. Mixed models contain both random and fixed effects; the mouse is the fixed effect, and replicates and dilutions are the random effects. The Benjamini-Hochberg corrected p-value < 0.05 with a false discovery rate (FDR) of 5% was considered for overall statistical significance across the entirety of the hypotheses. Results of all comparisons are provided in Appendix C (available from the authors).

Correlations among protein levels were determined by standard Spearman correlation analysis, with cutoffs for significance: correlation coefficient, $r>|0.80|$ and $p<0.05$. This test was chosen to assess the monotonic relationship between levels of two different proteins within the same set of mice; specifically here, it assesses the relationship between the levels of two different proteins within individuals in a single genotype-treatment group. If levels of two proteins are correlated, then as the levels of one protein increase when levels in individual mice are listed in rank order, the levels of the second protein also increase, or decrease (positive and negative correlations, respectively) in the same mice. An artefactually high r value can be generated when a protein dataset for a genotype-treatment group contains outliers or subgroups, or when low numbers of mice are associated with quality protein measurements. Scatter plots of all significant pairwise comparisons were manually reviewed and those with artefactually high r values were eliminated. Examples are provided in Figure 4.

Results

Proteins were measured in hippocampus from four groups of mice: two genotypes, trisomic Ts65Dn and euploid controls, and two treatments, vehicle and the $GABA_A\alpha5$ NAM, RO4938581. As described in Martinez-Cué et al. (2013), treatments were chronic, administered daily starting at 3-4 months of age, for 6 weeks before, and subsequently during, a behavior and learning/memory (LM) test battery that spanned a further 6 weeks. Protein profiles were thus generated from 6-7 month old mice and expression patterns reflect the combined effects of genotype, long term drug exposure and the stimulation and stress of the test battery. Groups are designated based on their performance in the MWM. In comparison with euploid controls, Ts65Dn treated with vehicle show impaired performance in the MWM and are designated as failed (F). Ts65Dn mice treated with RO4938581 show significantly improved performance

(although not to levels of controls) and are designated as partially rescued (R). Euploid control mice learn equally well with vehicle and RO4938581, and are considered to show normal learning (designated as N and NR, respectively). Protein expression analysis focused on between-group comparisons. While six pairwise comparisons are possible, four were of biological interest and are listed in Table 1.

Levels of 91 proteins were measured in the hippocampal samples. Twenty-seven measurements were to phosphorylation-specific, two were to acetylation-specific and the remainder were to modification-independent protein forms. A list of all the proteins can be found in Appendix B (available from the authors).

General features of the protein profiles

Table 2 summarizes, for each comparison, the number of proteins that differed between the two groups and the relative magnitudes of the differences. Two comparisons standout for the extent of the differences: FvN and RvF have 52 and 57 differences, respectively, compared to only 10 and 13 for RvN and NRvN. The magnitudes of the differences were also proportionately greater in FvN and RvF. In FvN, 30 of 52 differences were >20% (24 were increases and 6 were decreases) and in RvF, 37 of 57 differences were >20% (8 increases and 29 decreases). This is in contrast to only 4 of 10 and 2 of 13 differences >20% in RvN and NRvN.

Table 3 summarizes the number of proteins showing abnormal levels within six functional classes. The MAPK and MTOR pathways are well established for roles in LM and show many abnormalities in FvN and many responses to RO4938581 in RvF. In contrast, however, and consistent with improved and normal LM, respectively, there are many fewer differences in MAPK and MTOR components in RvN and NRvN. Also showing many trisomic perturbations and responses to RO4938581 are proteins related to NMDAR subunits and interactions, and AD-related proteins. Again, there are few differences in levels of these proteins in mice with improved and normal learning. Smaller numbers of immediate early gene (IEG) and apoptosis proteins were measured but these also show abnormalities in FvN that are normalized in response to successful learning (e.g. RvN).

Together, the data in Tables 2 and 3 indicate extensive abnormalities in protein expression in the Ts65Dn when they fail the MWM (FvN) and extensive responses to RO4938581 in the Ts65Dn when they then learn better in the MWM (RvF). Some of the former

responses may contribute to the LM failure, while some of the latter may contribute to the associated rescue of LM. Consistent with this, when the Ts65Dn learn better, the differences from controls in protein expression are reduced (RvN). RO4938581, however, is not without effects in control mice on components of MAPK and MTOR pathways, and NMDAR related proteins. Indeed, there are more differences in NRvN than in RvN. However, because NR mice learn normally, these differences either are not relevant to LM, are compensated by other changes, or the experimental protocol used to assess LM (MWM) was not able to detect subtle improvements in cognition in RO4938581 treated control mice.

The Venn diagram in Figure 2 illustrates common protein features among the four comparisons. Of the 91 proteins measured, only 23 did not differ in any comparison. Most notably, 44 proteins were affected in both FvN and RvF comparisons, and in all cases, the differences were opposite in direction. This indicates that RO4938581 tends to normalize levels of the proteins that are elevated or decreased in the Ts65Dn.

Hsa21 proteins

Due to dosage, trisomy is expected to lead to a 50% increase in expression levels of trisomic genes. As shown in Figure 3A, in the FvN comparison, this is indeed true: protein levels of trisomic genes APP, ITSN1, and RCAN1 are ~60% higher than controls, and those of DONSON, DYRK1A, SOD1, and TIAM1 are elevated by 20%-30%. Exceptions exist, however: the level of ETS2, that is trisomic, and the level of PRMT2, that is not trisomic (it maps to Mmu10), are both decreased by ~10%. There is no difference from controls in ADARB1 and RRP1 protein levels; these genes also map to Mmu10 and are not trisomic in the TS65Dn. The effects of RO4938581 on the Hsa21 orthologs are shown in Figures 3B and C. Unexpectedly, because the molecular mechanism relating a GABA receptor modulator to expression of these genes is completely unclear, levels of these proteins are largely normalized: decreased in the RvF comparison sufficiently that, with the exception of APP and SOD1, levels are not different from controls in RvN. Even the magnitude of the APP abnormality is reduced, from ~60% to only 10% greater than controls with RO4938581 treatment. However, in control mice, RO4938581 has no consequences for these same Hsa21 orthologs (Figure 3D).

NMDA Receptors and Related Proteins

Figure 3E-H shows a similar analysis of subunits of ionotropic glutamate receptors and functionally related proteins. As shown in Figure 3E, the NMDA receptor (NMDAR) subunits, NR1, NR2A, and NR2B, and their phosphorylated forms are repressed by ~20% in FvN. Subunits of the α-amino-3-hydroxy-5-methyl-4-isoxazolepropionic acid (AMPA) receptor are also decreased, as is the level of BDNF, a neurotrophic factor with a crucial role in neurogenesis. Only TRKA is elevated. Drug treatment reverses most of these abnormalities (Figure 3F) so that in RvN there are no significant differences in levels of any of these proteins. RO4938581 does, however, have some effects in control mice, increasing levels of pNR1, pNR2B and GLUR3.

Signaling pathways

Table 4 lists differences in MAPK and MTOR pathway components. Comparing columns 1 and 3 shows that RO4938581 normalizes most of the abnormalities seen in mice with impaired learning and residual differences tend to be small. Exceptions include, in both Ts65Dn and control mice treated with RO4938581, decreased levels of BRAF (-14% and -16%) and pERK (-24% and -23%) in RvN and NRvN. Specific to RvN is a decreased level of pAKT (-27%) and to NRvN, a decreased level of pS6 (-20%). Table 5 shows results of the same comparisons for IEG and AD-related proteins. RO4938581 normalizes the levels of CFOS and pCFOS, as well as levels of pTAU, pSRC and CHAT. Conversely, RO4938581 creates abnormalities in levels of ERBB4, decreasing levels by 14%-26%, in both Ts65Dn and controls. Also of interest are the responses to RO4938581 of the histone H3 modifications; specific to the Ts65Dn are decreases in levels of acetylation of H3 lysines 18 and 9.

Correlations among protein levels

The Ts65Dn are maintained by mating trisomic females to C57BL/6JEi x C3H/HeSnJ F1 hybrid males (Davisson et al.. 1990, 1993). At any locus therefore, euploid and trisomic individuals will have 0, 1 or 2 alleles from C57BL/6JEi and C3H/HeSnJ. The resulting sequence variation, depending on genomic location, can cause within-genotype, inter-individual variation in gene expression at the mRNA and protein levels. This has been reported previously at the protein level in naïve Ts65Dn where it was used to generate networks of correlated levels of functionally related proteins (Ahmed et al. 2012). To investigate possible consequences of genomic sequence variation in the current sets of mice, we carried out standard Spearman

correlation analysis for all pairs of proteins in euploid and trisomic mice, separately for vehicle and R04938581 treated groups.

Measurement of 91 proteins/protein modifications results in (91 X 90) ÷ 2, or ~4100, pairwise comparisons for each of the four genotype/treatment groups, for a total of ~16,000 comparisons. We retained as significant those with correlation coefficient $r > |0.80|$ and $p < 0.05$. For all significant correlations, scatter plots were reviewed for the presence of monotonic relationships between protein levels. Figures 4A-D show the relationships between levels of pNR1 and pNR2B. In 3 of 4 genotype/treatment comparisons, levels of both proteins increase monotonically. Strong correlations are present in both euploid controls and Ts65Dn treated with vehicle (Figure 4A,B). The correlation remains in drug treated Ts65Dn (Figure 4C, $r=0.87$, $p=0.004$), but is lost in RO4938581 treated controls (Figure 4D, $r=0.45$, $p=0.24$). Scatter plots in Figures 4E,F illustrate the strong correlations, in drug treated mice, between GAD2 and PP2A. In contrast, scatter plots in Figure 4G and H illustrate correlations that meet the numerical criteria but that were eliminated because of potential artifacts. In Figure 4G, while the r value is high ($r=0.96$), the data in vehicle treated controls appear in two clusters, suggesting the possibility of two groups of mice, one with low values of both DYRK1A and RCAN1 and the other with high values of both proteins. In Figure 4H, the relationship between pNR2A and CFOS in vehicle treated Ts65Dn is ambiguous; while the r value is high, there are again possibly different groups of mice, one group where pNR2A levels increase while CFOS levels are relatively constant and one where pNR2A levels remain constant while CFOS levels increase. Increasing the number of individuals in each group would resolve the kinds of ambiguities seen in Figures 4G,H. For purposes here, however, we used stringent criteria and retained only those correlations showing no potential artefacts.

Within each treatment group, correlations included some that were specific to either euploid controls or Ts65Dn and some that were common to both genotypes. After manual review of scatter plots and elimination of those with artefactual significance (see Methods), two features of the final set of correlations were evident. First, in vehicle-treated mice, the Ts65Dn frequently have much larger numbers of correlated proteins than do euploid controls. For example, as shown in Table 6, in the Ts65Dn, CFOS and pGLUR2 are correlated with 18 and 19 proteins, respectively, while in euploid controls they are correlated with only 4 proteins each (total correlations for a genotype-treatment are the sum of the number of correlations common to both

genotypes plus the number of correlations that are genotype specific). Second, for most proteins, many correlations seen in vehicle treated Ts65Dn mice, including both those in common with controls and those specific to Ts65Dn, are lost in R04938581 treated mice, while few new correlations appear. For example, CFOS correlations are reduced from 18 to 2 in Ts65Dn and those for pGLUR2 are reduced from 19 to 7 (Table 6).

Patterns of correlations among proteins can be illustrated as networks. Examples for selected proteins are shown in Figures 5 and 6 (although some proteins are present in both figures, the networks are shown separately for clarity). Figure 5 illustrates networks involving subunits of ionotropic glutamate receptors. For each of three NMDAR subunits, NR1, NR2A and NR2B, one phosphorylation-independent and one phosphorylation-dependent form were measured. Figure 5A shows that, in vehicle treated mice, levels of five of these forms are correlated in 8 pairwise comparisons that are common to both euploid controls and Ts65Dn. Of the three AMPAR subunits measured, uniquely in the Ts65Dn, levels of pGLUR2 are correlated with each of the five NMDAR subunits, while correlated only with GLUR4 in euploid controls. Figures 5B,C show the networks in RO4938581 treated mice. Of the correlations among NMDAR subunits, only 2 remain in euploid mice, between pNR1 and NR2A and NR2B. Conversely, in Ts65Dn, 7 of 8 common correlations remain, with only that between NR1 and pNR1 lost. Unique to the Ts65Dn is the number of correlations between NMDAR and GLUR4 and BDNF. Additional correlations involve GAD2 (glutamic acid decarboxylase), of interest because it catalyzes the production of gamma-aminobutyric acid from L-glutamic acid. Common to both genotypes are new correlations between GAD2 and pGLUR2 and GLUR4, and between pGLUR2 and GLUR3.

Networks involving the serine-threonine protein phosphatase, PP2A, PPP2R1A subunit, are shown in Figure 6. PP2A functions in regulation of MAPK and AKT signaling and among its targets are Tau, GSK3B and DYRK1A. PP2A, and its networks, are among the minority of proteins where the number of correlations common to euploid and Ts65Dn increases, rather than decreases, with drug treatment. In vehicle treated mice (Figure 6A), there are common correlations involving 4 proteins, 3 of which are between PP2A and pGLUR2, GFAP and RSK. In drug treated mice (Figure 6B), the network is much more dense; there are 13 common correlations, involving 7 proteins; 6 correlations involve PP2A. Some of these new common correlations were genotype-specific in vehicle treated mice, however, the Ts65Dn-specific

correlations seen in vehicle treated mice involving NMDAR subunits, DYRK1A and ARC are lost. Drug induced correlations again include GAD2, and those with PP2A and RSK are common to both genotypes.

Discussion

Levels of 91 proteins/protein modifications were measured in hippocampus of Ts65Dn and littermate control mice after exposure to a battery of behavioral and LM tests, with and without chronic treatment with the $GABA_A\alpha5$ NAM, RO4938581. The diversity of proteins measured reveals the complexity in the Ts65Dn of both the initial perturbations and the responses to the drug, and the relationships between these data sets. Most notably, of the 52 proteins showing abnormal levels in the vehicle treated Ts65Dn, 44 responded to RO4938581 with direction and magnitudes of changes that largely tended to normalize these protein levels. These proteins include several encoded by Hsa21, levels and activation of components of the MAPK and MTOR pathways, IEG proteins, subunits of ionotropic glutamate receptors and AD-related proteins. While each of these pathways and processes has well established relevance to LM, the direct molecular mechanisms relating their responses to $GABA_A$ signaling, and its inhibition, and to the functions of Hsa21 genes, are not known and normalization of such a broad range of proteins was unexpected.

RO4938581 binds directly to the α5 subunit of the $GABA_A$ receptor. No transcription factors, and indeed no other proteins, are known to be targets. However, RO4938581 treatment may indirectly result in changes in transcription or protein post translational modifications, first because RO4938581 binding is known to reduce inhibition. The associated increase in excitatory neurotransmission will result in activity-dependent plasticity which activates transcription of many genes (Flavell and Greenberg, 2008). In addition, because $GABA_A$ α5 receptors are localized at dendrites of pyramidal cells in close proximity to NMDA receptors, inhibition of $GABA_A$ receptor activity may contribute to activation of NMDA receptors, with consequent downstream responses in signaling pathways.

Measurement of mRNA levels, by qPCR, microarrays or sequencing, in Ts65Dn with and without drug treatment, would determine if RO4938581 represses transcription of the trisomic genes APP, SOD1, ITSN1, DYRK1A and RCAN1. Each of these Hsa21 orthologs is well established to contribute to the trisomy phenotype in mouse models of DS and each is commonly

found to be elevated in tissues from DS and mouse models (Vilardell et al 2011). If normalization of mRNA levels underlies the observed normalization of protein levels found here, further studies would be needed to determine the mechanisms of such regulation, i.e. is direct repression of trisomic gene transcription caused by altered levels or activation of necessary transcription factors, or more indirectly, are mRNA levels reduced due to increased rates of degradation? However, mRNA levels do not reliably predict protein levels (Schwanhausser et al. 2011; Vogel and Marcotte 2011). Therefore, normalization of protein levels does not require RO4938581 to influence transcription. Alternatively, it may negatively affect efficiency of translation or protein stability.

In the prior Ts65Dn report, Martinez-Cué et al (2013) showed that RO4938581 treatment rescued multiple abnormalities in synaptic plasticity and cellular features that have been well established in untreated Ts65Dn (Insausti et al., 1998; Rueda et al., 2005; Clark et al., 2006; Lorenzi and Reeves, 2006; Bianchi et al., 2010; Llorens-Martín et al., 2010). This included rescue of deficits in adult neuronal proliferation and survival, and normalization of LTP. $GABA_A$ receptor activity has been shown to regulate neuronal proliferation, migration, differentiation, and integration of newly generated neurons (Tozuka et al., 2005; Ge et al., 2006; Earnheart et al., 2007; Song et al., 2012). Because both newborn and mature neurons are implicated in hippocampus dependent learning and memory, the restoration of proliferation and the density of mature neurons is likely to be involved in the cognitive-enhancing effects of RO4938581 in TS mice. Furthermore, the correction by RO4938581 treatment of abnormal expression of glutamate receptors subunits may also contribute to reducing the over-inhibition and hence rescuing LTP.

Comparison with prior Ts65Dn expression studies

Braudeau et al. (2011a) measured responses by microarrays and qPCR to treatment with the partial inverse agonist, 3-(5-methylisoxazol-3-yl)-6-[(1-methyl-1,2, 3-triazol-4-yl)methyloxy]-1, 2, 4-triazolo[3, 4-a]phthalazine (α5IA). In hippocampus of vehicle treated Ts65Dn mice, levels of ITSN1 and SOD1 were elevated, consistent with protein results here. In contrast, levels of APP, TIAM1, RCAN1 or DYRK1A did not differ from euploids, while here each was significantly elevated at the protein level. α5IA rescued the Ts65Dn impairments in learning in the MWM and also normalized SOD1 mRNA levels; this normalization did not occur

at the protein level with RO4938581. That mRNA levels do not reliably predict protein levels (Schwanhausser et al. 2011; Vogel and Marcotte 2012) may account for these disparate results.

For non-Hsa21 orthologs, Braudeau et al. (2011a) reported significantly reduced CFOS in hippocampus of vehicle treated Ts65Dn relative to controls, and normalization of these levels after treatment with α5IA; similar increases in CFOS were also seen in controls. At the protein level, Braudeau et al. (2011b) measured CFOS immunostaining in the dentate gyrus and CA1 region of the hippocampus after acquisition in the NOR. Levels did not differ between vehicle treated Ts65Dn and controls, in contrast to the authors' mRNA data (Braudeau et al. 2011a), nor between α5IA treated Ts65Dn and controls. Again, these results partially agree with those found here: the CFOS protein level was reduced relative to controls in Ts65Dn vehicle treated mice, and RO4938581 treatment normalized the CFOS level, without affecting that in controls.

At least some of the differences in results likely reflect differences in experimental paradigms. Here, mice were subjected to a battery of behavioral and LM tests, and administered RO4938581 for 6 weeks prior to, and for an additional 6 weeks during, testing. In contrast, in Braudeau et al. (2011a,b), mice were exposed only to a single test, either the MWM or NOR, and were treated with α5IA for shorter periods of time, in the NOR experiments, with a single dose (Braudeau et al. 2011b). Differences in the amount of handling, and the stress and stimulation associated with a series of evaluations, versus a single one, may also contribute to gene expression differences. This is well illustrated by considering results from a comprehensive analysis of protein expression in naïve Ts65Dn mice reported in Ahmed et al (2012). Vehicle treated Ts65Dn mice here show a very different profile of abnormalities from those seen in Ahmed et al (2012). These affect both Hsa21 orthologs, e.g. TIAM1, that was not elevated in hippocampus of naïve Ts65Dn, and non-Hsa21 orthologs (data not shown). A thorough exploration of these differences should help to understand the molecular basis of Ts65Dn impairments and will be reported in the future.

Correlation networks

Protein correlations present a novel view of molecular events in LM and drug responses. The biological significance, however, of correlations and their associated networks, remains to be determined and there is evidence both for and against it. Support for biological relevance is the observation of correlated levels among proteins known to form a functional complex. In such

cases, correlated levels might reflect the need to maintain specific levels of each component to correctly assemble and regulate the activity of the complex. One example, in vehicle treated euploid mice, involves the highly correlated levels of NMDAR subunits, where 5 of the 6 proteins are present in a network of 8 pairs (Figure 3A). On the other hand, in RO4938581 treated euploid mice, 6 of these correlations are lost. Euploid mice perform and learn the sets of tasks equally well with and without the drug. This argues against the biological relevance, for the behaviors and tasks examined here, of the specific correlations among NMDAR subunits.

Interpretation of the biological relevance is further complicated by observations in Ts65Dn. Correlations among NMDAR subunits in vehicle treated Ts65Dn are similar to those in euploid mice. This differs from results of a prior analysis of naïve mice, where Ts65Dn had many fewer correlations than euploid littermates among these same proteins (Ahmed et al. 2012). In that work, it was argued that the absence of correlated levels in trisomy might contribute to neurological abnormalities. The age of mice in Ahmed et al. (2012) was similar to that of mice here. It is possible, therefore, that the stimulation of daily exposure to handling, novelty and the MWM experienced by the mice here, induces changes in relative protein levels to result in correlated values. That the vehicle treated Ts65Dn network appears similar to euploids suggests that some normal responses occur with the stimulation to learn, in spite of the impairment in performance. In drug treated Ts65Dn mice, the majority of correlations among NMDAR subunits remain, in contrast to their loss in drug treated euploid mice. The presence and persistence of correlations between NMDAR subunits and BDNF and AMPA subunits uniquely in the Ts65Dn needs to be explored for relevance to molecular mechanisms that may contribute to or compensate for abnormal responses to stimulation.

Correlations do not necessarily reflect known physical associations. This is illustrated in PP2A-PPP2R1A subunit networks. The PP2A protein phosphatase is a multi-subunit complex, composed of catalytic, regulatory and scaffolding subunits. There are multiple genes encoding each type of subunit, leading to considerable diversity in PP2A holoenzyme composition, and consequent diversity in activity level and substrate specificities and affinities (reviewed in Nematullah et al. 2017; Kiely and Kiely 2015). Because only the regulatory subunit PPP2R1A was measured here, only a partial view of PP2A relationships is generated. To interpret the PP2A network, we considered both protein interaction partners and substrates. Of >300 interaction partners identified for PPP2R1A (NCBI Gene #2538), NR1 and AKT were measured here, and

of known substrates, DYRK1A, TAU, AKT and MAPK components were measured. Of these, NR1 (only the phosphorylated form) and DYRK1A levels were correlated with PP2A in the vehicle treated, but not drug treated, Ts65Dn, and the MAPK component RSK was correlated in both genotypes and treatments. That the PP2A networks involve a number of other proteins, therefore, may indicate novel interaction partners, substrates of the PPP2R1A subunit, unknown indirect functional relationships, or merely curious artefacts.

An additional network feature, after RO4938581 treatment, is the appearance of GAD2 in common and genotype specific correlations. These novel correlations may be explained by the target and mechanism of action of RO4938581. RO4958381 binds to the GABAAα5 subunit and negatively modulates activity of the receptor. The majority of $GABA_A$α5 receptors are localized extrasynaptically and mediate tonic inhibition in response to extracellular ambient GABA (Serwanski et al. 2006). It has been suggested that changes in the activity of synaptic and extrasynaptic $GABA_A$ receptors might impact GAD2 activity, thus, indirectly influencing GABA synthesis and release (Blednov et al. 2010). GABAergic activity is elevated in the vehicle treated Ts65Dn (Martinez-Cué et al. 2013), and the level of GAD2, which regulates GABA synthesis, is repressed, a reasonable compensatory response to over inhibition. In these conditions, GAD2 levels are not correlated with any proteins. Because GABAergic synapses adjust their strength depending on the pattern of neuronal activity (Melle et al. 2016), the RO4938581-induced reduction in $GABA_A$α5 receptor activation might be predicted to impact the synthesis of GABA by normalizing GAD2 expression. This is indeed observed in the Ts65Dn when inhibition is corrected by RO4938581 treatment. This is, however, a genotype-specific correction, because it is not observed in euploid controls. The correlations induced by RO4938581 between GAD2 and AMPA receptor subunits occur in both genotypes. In the Ts65Dn, additional correlations are induced between GAD2 and BDNF, and between GAD2 and phosphorylated forms of NMDAR subunits, possibly reflecting mechanisms underlying rescue of the imbalance between excitatory and inhibitory neurotransmission that occurs specifically in these mice. Further study is required to determine the biological significance and if there exist molecular mechanisms connecting GAD2, RO4938581 and components of the correlation networks.

No correlations were observed between any parameter of MWM performance and the levels of any protein, either in euploid controls or Ts65Dn, in vehicle or drug treated mice. This is not surprising given the complexity of learning and memory. It is also consistent with a

previous analysis of protein responses in the Ts65Dn subjected to context fear conditioning, with and without treatment with the NMDA receptor modulator, memantine (Ahmed et al 2014, 2015). A more sophisticated bioinformatics approach, using Self-Organizing Feature Maps (SOM), was, however, successful in identifying patterns in protein expression that distinguished successful learning, in vehicle or drug treated controls and drug treated Ts65Dn, from failed learning, in vehicle treated Ts65Dn (Higuera et al. 2015). A similar analysis is in progress with data from RO4938581 experiments.

LTP Pathway

Long term potentiation is considered to be a cellular mechanism underlying synaptic plasticity and LM. Several studies have shown repressed hippocampal LTP in the Ts65Dn (Siarey et al. 1997; Kleschevnikov et al. 2004) and treatment with RO4938581 increased LTP in Ts65Dn hippocampus to levels not different from untreated controls (Martinez-Cué et al. 2013). To gain insight into the molecular basis of this rescue, we superimposed RPPA data onto the curated LTP protein pathway from the KEGG database. The pathway was expanded with protein interaction partners known to be expressed in brain. Results are shown in Figure 7, with each node color-coded for perturbation and response to RO4938581 in the Ts65Dn. Including both modification dependent and independent protein forms, a total of 64 proteins, comprising 24 pathway components and 40 interacting proteins, were measured. Thirteen were unaffected by genotype or treatment (shown in grey), and 51 were perturbed in the Ts65Dn (FvN, in yellow), a proportion that is consistent with the observation of perturbed LTP. After drug treatment, however, there remain only 8 protein abnormalities (RvN, in green): three pathway components, CAMKIIα/β, BRAF, and pERK1/2, and five interactors, pAKT, APP, ERBB4 and two histone H3 lysine-acetylated forms. This striking decrease in complexity of protein abnormalities is consistent with the rescue of repressed LTP, however, this same complexity makes it difficult to interpret the molecular mechanisms of RO4938581. The protein abnormalities that are present in the vehicle treated Ts65Dn and that are resolved by RO4938581 likely include two types: (i) abnormalities that contribute to the LTP defects, or that lie directly downstream of these, and respond to RO4938581 inhibition of $GABA_A\alpha5$, and (ii) abnormalities that do not contribute to repressed LTP, but rather that were induced as compensation for the trisomic perturbations. The latter abnormalities are eliminated by the removal of the initial perturbations. It remains to be

determined which proteins belong to each category. This would discriminate those abnormalities that are critical to correct from those that, conversely, if removed, would likely exacerbate the functional impairment by removing compensatory abnormalities.

The molecular basis of pharmacological rescue of LM after RO4938581 treatment

More than 20 drugs, small molecules and nutritional supplements have been shown to rescue impaired performance in the Ts65Dn in at least one LM task (reviewed in Gardiner 2009, 2014; Das and Reeves 2011). Most of these studies used adult mice (Gardiner 2014), suggesting that it might be possible to improve cognitive abilities in a large proportion of people with DS, i.e. the data suggest that the postnatal, even adult, brain is sufficiently plastic for significant LM improvement. A confounding, but interesting, factor is the diversity of targets and mechanisms of action of the successful treatments. This fact is often not mentioned in reports of new successful treatments nor in limited reviews of the topic (Das et al. 2014), but failing to consider it may hamper progress toward effective treatments. Exploiting the diversity of successful drug properties to build understanding of the molecular basis of LM rescue could lead to rational proposals of new drug targets or creation of a cocktail of drugs that is more effective than any single drug. Given the very modest (and negative) results of clinical trials with single drugs based on LM evaluations in the Ts65Dn (Boada et al. 2012; Hanney et al. 2012; Lott et al. 2011; de la Torre et al. 2016), pursuing new drug targets or cocktails of drugs are reasonable additions to proposals of larger trials, longer trials and inclusion of younger participants.

In previous work, we examined protein expression changes in response to an NMDAR inhibitor, memantine (Ahmed et al. 2015). This allows comparison of the responses to inhibition of inhibitory neurotransmission by RO4938581 with those of inhibition of excitatory neurotransmission by memantine. There are significant differences in experimental protocols. Memantine treatment was acute and mice were exposed to a single task, context fear conditioning (CFC) (Ahmed et al. 2015), while RO4938581 treatment was chronic, and mice were exposed to multiple behavioral assessments and then the MWM. In addition, memantine treated mice were sacrificed 60 minutes after training in CFC. This time point was chosen specifically to capture protein responses known to be required for LM in CFC and to occur within that time frame, such as MAPK components and IEG proteins (Atkins et al. 1998; Ahmed et al. 2014; Ivashkina et al. 2016). In contrast, RO4938581 treated mice were sacrificed 24 hours

after the last of several days of training in the MWM. The timing with respect to molecular responses required for LM in the MWM is not known, but given the incremental improvements in learning seen in sequential training sessions, the time frame is unlikely to be discrete. Protein profiles likely also reflect chronic responses to drug treatment, and not specifically LM. Lastly, the memantine data were generated from subcellular fractions of the hippocampus (nuclear, cytosolic and membrane), while the RO4938581 data were generated from whole hippocampus lysates.

In Figure 8, we summarize protein expression in the Ts65Dn in two comparisons with normal LM in controls: when Ts65Dn fail to learn and when Ts65Dn successfully learn, i.e. the FvN and RvN comparisons. In the memantine experiments, the comparisons corresponding to FvN and RvN are, respectively, the context-shock (CS)-saline Ts65Dn vs. CS-saline controls and the CS-memantine Ts65Dn vs. CS saline controls. Figure 8A shows data for 19 proteins with localization to the membrane and the cytosol. These include Hsa21 proteins and NMDAR and AMPAR subunits. The FvN comparisons show that the two LM protocols result in different profiles of protein perturbations in the Ts65Dn that fail to learn the respective tasks; this is not unexpected from the differences in extent, timing and type of LM stimulation. Perturbations in vehicle treated Ts65Dn from the RO4938581 experiment show largely repressed levels while those from the memantine experiment include elevated levels in both the cytosol and membrane. In the RvN data, RO4938581 completely normalizes levels of these proteins, while memantine fails to normalize Hsa21 encoded proteins DYRK1A, ITSN1 and TIAM1, as well as elevated levels of NR2A and NR2B. In Figure 8B, proteins with cytosolic and nuclear localization are shown. The perturbations in the FvN are again quite different between the two LM protocols. Those from the battery of tests show 37 abnormalities, largely elevated, while those from only CFC show 13 and 11 abnormalities in the nuclear and cytosol fractions, respectively. The RvN comparisons in Figure 8B show that RO4938581 results in correction of 32 of the abnormalities in impaired LM. Elevated levels of APP or SOD1 remain and there is over compensation in levels of BRAF, pERK and STAT3 that now are decreased relative to controls. Memantine largely corrected nuclear abnormalities, but was less effective in normalizing cytosolic levels. Notably unaffected by memantine were abnormal levels of most of the Hsa21 encoded proteins.

Differences in protein profiles likely include some related to the molecular processes required for different types of learning, e.g. spatial learning in the MWM vs. associative learning

in CFC. It would be useful, however, if they could be used predict impaired performance and drug-induced rescue of performance in a range of LM tasks. It is notable that RO4938581 failed to correct impairment in CFC (Martinez-Cué, unpublished), while memantine was successful in rescue of MWM performance (Rueda et al. 2010). Differences in efficacy in rescue of specific LM tasks are not unique to RO4938581; they have been noted in several drug treatments of the Ts65Dn, e.g. the GABAB receptor antagonist, CGP55845, rescued performance in object recognition, but not in CFC, lithium rescued performance in CFC but not in the T-maze, and the Sonic Hedgehog analog, SAG.1. rescued performance in the MWM but in not the Y-maze. Comparing protein profiles after each LM task, with and without treatment with individual drugs, would help to discriminate normal task-specific responses and those critical to rescue of specific Ts65Dn impairments. In this way, protein expression data, could be used to identify drugs with efficacy against a broad range of LM tasks or cocktails of drugs, each effective in rescuing different tasks.

This study corroborates extensive abnormalities in protein expression in hippocampus of Ts65Dn mice that may contribute to their neurological deficits. Chronic RO4938581 treatment rescued most of the molecular abnormalities and many of these deficits. The proteins measured included, not only several encoded by Hsa21, but also a broad range of proteins of known importance to brain development and function, thus supporting the argument that these molecular changes are implicated in the enhanced LM, neurogenesis and LTP found in Ts65Dn mice after chronic administration of this NAM. To deconvolute the molecular responses required for rescue in the Ts65Dn, additional studies are needed, using consistent LM protocols and comparing additional drugs. This is a complicated project and one needing replication in additional mouse models of DS, to account for contributions to the DS phenotype of trisomy all Hsa21 orthologs. Given the expense, and failures, of clinical trials for ID in DS, devoting time and effort to understanding molecular correlates may be advantageous.

Acknowledgements

This work was supported by the National Institutes of Health [HD056235]; the Linda Crnic Institute for Down Syndrome; the Jérôme Lejeune Foundation; the Fundación Tatiana Pérez de

Guzmán el Bueno and the Spanish Ministry of Economy and Competitiveness [PSI2016-76194-R/AEI/FEDER/UE].

References

Ahmed MM, and Gardiner KJ (2011), Preserving protein profiles in tissue samples: differing outcomes with and without heat stabilization. J Neurosci.Methods,196: 99-106.

Ahmed M, Sturgeon X, Ellison M, Davisson MT, Gardiner KJ (2012), Loss of correlations among proteins in brains of the Ts65Dn mouse model of down syndrome. J Proteome Res 11:1251-1263.

Ahmed MM, Dhanasekaran AR, Tong S, Wiseman FK., Fsher EM, Tybulewicz VL, Gardiner KJ (2013), Protein profiles in Tc1 mice implicate novel pathway perturbations in the Down syndrome brain. Hum Mol Genet 22:1709-24.

Ahmed MM, Dhanasekaran AR, Block A, Tong S, Costa AC, Gardiner KJ (2014), Protein profiles associated with context fear conditioning and their modulation by memantine. Mol Cell Proteomics 13:919-37.

Ahmed MM, Dhanasekaran AR, Block A, Tong S, Costa AC, Stasko M, Gardiner KJ (2015), Protein dynamics associated with failed and rescued learning in the Ts65Dn mouse model of Down syndrome PLoS One 10:e0119491.

Atkins CM, Selcher JC, Petraitis JJ, Trzaskos JM, Sweatt JD (1998), The MAPK cascade is required for mammalian associative learning. Nat Neurosci. 1:602-609.

Ballard TM, Knoflach F. Prinssen E, Borroni E, Vivian JA, Basile J, Gasser R, Moreau JL, Wettstein JG, Buettelmann B, Knust H, Thomas AW, Trube G, Hernandez MC (2009), RO4938581, a novel cognitive enhancer acting at GABAA a5 subunit-containing receptors. Psychopharmacol 202: 207-223.

Bianchi P, Ciani E, Guidi S, Trazzi S, Felice D, Grossi G, Fernandez M, Giuliani A, Calza L, Bartesaghi R. (2010) Early pharmacotherapy restores neurogenesis and cognitive performance in the Ts65Dn mouse model for Down syndrome. J Neurosci. 30:8769–8779.

Bittles AH, Glasson EJ (2004), Clinical, social, and ethical implications of changing life expectancy in Down syndrome. Dev Med Child Neurol 46:282-286.

Bittles AH, Bower C, Hussain R, Glasson EJ (2007), The four ages of Down syndrome. Eur J Public Health 17:221-225.

Blednov YA, Walker DL, Iyer SV, Homanics G, Harris AR (2010), Mice lacking Gad2 show altered behavioral effects of ethanol, flurazepam and gabaxadol. Addict Biol 15:45-61.

Block A, Dhanasekaran AR, Ahmed MD, Gardiner KJ (2014), Abnormal protein profiles in hippocampus of mouse models of Down syndrome: similarities with Alzheimer's Disease. J Alzheimer's Disease and Parkinsonism 4:138-149.

Boada R, Hutaff-Lee C, Schrader A, Weitzenkamp D, Benke TA, et al. (2012), Antagonism of NMDA receptors as a potential treatment for Down syndrome: a pilot randomized controlled trial. Transl Psychiatry 2: e141.

Braudeau J, Dauphinot L, Duchon A, Loistron A, Dodd RH, Hérault Y, Delatour B, Potier MC (2011), Chronic Treatment with a Promnesiant GABA-A α5-Selective Inverse Agonist Increases Immediate Early Genes Expression during Memory Processing in Mice and Rectifies Their Expression Levels in a Down Syndrome Mouse Model. Adv Pharmacol Sci 2011:153218.

Braudeau J, Delatour B, Duchon A, Pereira PL, Dauphinot L, de Chaumont F, Olivo-Marin JC, Dodd RH, Hérault Y, Potier MC (2011b), Specific targeting of the GABA-A receptor α5 subtype by a selective inverse agonist restores cognitive deficits in Down syndrome mice. J Psychopharmacol 25:1030-1042.

Busciglio J, Yankner BA (1995), Apoptosis and increased generation of reactive oxygen species in Down's syndrome neurons in vitro. Nature 378:776-779.

CDC, Centers for Disease Control and Prevention (2006), Improved National Prevalence Estimates for 18 Major Birth Defects, MMWR 54:6-12.

Chapman RS, Hesketh LJ.(2000) Behavioral phenotype of individuals with Down syndrome. Ment Retard Dev Disabil Res Rev 6: 84-95.

Choong XY, Tosh JL, Pulford LJ, Fisher EM (2015), Dissecting Alzheimer disease in Down syndrome using mouse models. Front Behav Neurosci 9:268

Clark S, Schwalbe J, Stasko MR, Yarowsky PJ, and Costa ACS (2006), Fluoxetine rescues deficient neurogenesis in hippocampus of the mouse model for Down syndrome Ts65Dn. Exp Neurol 200:256-261.

Coskun PE, Busciglio J (2012), Oxidative Stress and Mitochondrial Dysfunction in Down's Syndrome: Relevance to Aging and Dementia. Curr Gerontol Geriatr Res 2012:383170.

Costa AC, Scott-McKean JJ, Stasko MR (2008), Acute injections of the NMDA receptor antagonist memantine rescue performance deficits of the Ts65Dn mouse model of Down syndrome on a fear conditioning test. Neuropsychopharmacology 33:1624-1632.

Das D, Phillips C, Hsieh W, Sumanth K, Dang V, Salehi A (2014), Neurotransmitter-based strategies for the treatment of cognitive dysfunction in Down syndrome. Prog Neuropsychopharmacol Biol Psychiatry 54:140-148.

Das I, Park JM, Shin JH, et al. (2013), Hedgehog agonist therapy corrects structural and cognitive deficits in a Down syndrome mouse model. Sci Transl Med. 5:201ra120

Das I, Reeves RH (2011), The use of mouse models to understand and improve cognitive deficits in Down syndrome. Dis Model Mech 4:596-606.

Davisson MT, Schmidt C, and Akeson E (1990), Segmental trisomy of murine chromosome 16: a new model system for studying Down syndrome. Progress in Clinical and Biological Research 360:263-280

Davisson MT, Schmidt C, Reeves RH, Irving NG, Akeson EC et al. (1993), Segmental trisomy as a mouse model for Down syndrome. Prog Clin Biol Res 384: 117-133.

de Graaf G, Buckley F, Skotko BG (2016), Estimation of the number of people with Down syndrome in the United States. Genet Med 2016 Sep 8.

De la Torre R, de Sola S, Hernandez G, Farré M, Pujol J, Rodriguez J, Espadaler JM, Langohr K, Cuenca-Royo A, Principe A, Xicota L, Janel N, Catuara-Solarz S, Sanchez-Benavides G, Bléhaut H, Dueñas-Espín I, Del Hoyo L, Benejam B, Blanco-Hinojo L, Videla S, Fitó M, Delabar JM, Dierssen M; TESDAD study group (2016), Safety and efficacy of cognitive training plus epigallocatechin-3-gallate in young adults with Down's syndrome (TESDAD): a double-blind, randomised, placebo-controlled, phase 2 trial. Lancet Neurol 15:801-810.

Earnheart JC, Schweizer C, Crestani F, Iwasato T, Itohara S, Mohler H, Luscher B. (2007) GABAergic control of adult hippocampal neurogenesis in relation to behavior indicative of trait anxiety and depression states. J Neurosci. 27:3845–3854.

Espina V, Wulfkuhle JD, Calvert VS, Petricoin EF 3rd, Liotta LA. (2007) Reverse phase protein microarrays for monitoring biological responses. Methods Mol Biol. 383:321-36.

Fernandez F, Morishita W, Zuniga E, et al. (2007), Pharmacotherapy for cognitive impairment in a mouse model of Down syndrome. Nat Neurosci 10:411-413.

Flavell SW, Greenberg ME (2008). Signaling mechanisms linking neuronal activity to gene expression and plasticity of the nervous system. Annu. Rev. Neurosci. 31: 563–90.

Gardiner K (2009), Pharmacotherapies for cognition in Down syndrome. Trends in Pharm Sci 32:66-73.

Gardiner KJ (2014), Pharmacological approaches to improving cognitive function in Down syndrome: current status and considerations. Drug Des Devel Ther 9:103-125.

Ge S, Goh EL, Sailor KA, Kitabatake Y, Ming GL, Song H. (2006) GABA regulates synaptic integration of newly generated neurons in the adult brain. Nature. 439:589 –593.

Glasson EJ, Sullivan SG, Hussain R, Petterson BA, Montgomery PD, Bittles AH (2002), The changing survival profile of people with Down's syndrome: implications for genetic counselling. Clin Genet 62:390-393.

Glasson EJ, Jacques A, Wong K, Bourke J, Leonard H (2016,) Improved Survival in Down Syndrome over the Last 60 Years and the Impact of Perinatal Factors in Recent Decades. J Pediatr 169:214-220.

Gupta M, Dhanasekaran A, Gardiner KJ (2016), Mouse models of Down syndrome: gene content and consequences. Mamm Genome 27:538-555.

Hanney M, Prasher V, Williams N, Jones EL, Aarsland D, et al (2012), Memantine for dementia in adults older than 40 years with Down's syndrome (MEADOWS): a randomised, double-blind, placebo-controlled trial. Lancet 379: 528-536.

Herault Y, Duchon A, Velot E, Marechal D, Brault V (2012), The in vivo Down syndrome genomic library in mouse. Prog Brain Res 197:169-197

Higuera C, Gardiner KJ, Cios KJ (2015), Self-Organizing Feature Maps Identify Proteins Critical to Learning in a Mouse Model of Down Syndrome. PLoS One 10:e0129126.

Holtzman DM, Santucci D, Kilbridge J, Chua-Couzens J, Fontana DJ, Daniels SE, …., Mobley WC (1996), Developmental abnormalities and age-related neurodegeneration in a mouse model of Down syndrome. Proc Natl Acad Sci U S A 93:13333-13338.

Hunter CL, Bachman D, Granholm AC (2004), Minocycline prevents cholinergic loss in a mouse model of Down's syndrome. Ann Neurol 56:675-688.

Insausti AM, Megías M, Crespo D, Cruz-Orive LM, Dierssen M, Vallina IF, Insausti R, Floro´ z J, Vallina TF (1998). Hippocampal volume and neuronal number in Ts65Dn mice: a murine model of Down syndrome. Neurosci Lett. 253:175–178.

Inglis A, Lohn Z, Austin JC, Hippman C (2014), A 'cure' for Down syndrome: what do parents want? Clin Genet 86:310-317.

Irving C, Basu A, Richmond S, Burn , and Wren C (2008), Twenty-year trends in prevalence and survival of Down syndrome. Eur J Hum Genet 16:1336-1340.

Ivashkina OI, Toropova KA, Ivanov AA, Chekhov SA, Anokhin KV (2016), Waves of c-Fos and Arc Proteins Expression in Neuronal Populations of the Hippocampus in Response to a Single Episode of New Experience. Bull Exp Biol Med 160:729-732.

Karmiloff-Smith A, Al-Janabi T, D'Souza H, Groet J, Massand E, Mok K, Startin C, Fisher E, Hardy J, Nizetic D, Tybulewicz V, Strydom A (2016), The importance of understanding individual differences in Down syndrome. F1000Res. 5. pii: F1000 Faculty Rev-389.

Kiely M, Kiely PA (2015), PP2A: The Wolf in Sheep's Clothing? Cancers (Basel) 7:648-69.

Kleschevnikov AM, Belichenko PV, Villar AJ, Epstein CJ, Malenka RC, Mobley WC (2004), Hippocampal long-term potentiation suppressed by increased inhibition in the Ts65Dn mouse, a genetic model of Down syndrome. J Neurosci 24:8153-8160.

Kucik JE, Shin M, Siffel C, Marengo L, Correa A (2013), Congenital Anomaly Multistate Prevalence and Survival Collaborative. Trends in survival among children with Down syndrome in 10 regions of the United States. Pediatrics. 131:e27-36.

Liu D P, Schmidt C, Billings T, Davisson MT (2003), Quantitative PCR genotyping assay for the Ts65Dn mouse model of Down syndrome. Biotechniques 35:1170-1174.

Llorens-Martín MV, Rueda N, Tejeda GS, Flórez J, Trejo JL, Martínez-Cué C. (2010) Effects of voluntary physical exercise on adult hippocampal neurogenesis and behavior of Ts65Dn mice, a model of Down syndrome. Neuroscience. 171:1228 –1240.

Lockrow J, Boger H, Bimonte-Nelson H, Granholm AC (2011), Effects of long-term memantine on memory and neuropathology in Ts65Dn mice, a model for Down syndrome. Behav Brain Res 221:610-22.

Lockrow J, Prakasam A, Huang P, Bimonte-Nelson H, Sambamurti K, Granholm AC (2009), Cholinergic degeneration and memory loss delayed by vitamin E in a Down syndrome mouse model. Exp Neurol 216: 278-289.

Lorenzi HA, Reeves RH. (2006) Hippocampal hypocellularity in the Ts65Dn mouse originates early in development. Brain Res. 1104:153–159.

Lott IT, Doran E, Nguyen VQ, Tournay A, Head E, Gillen DL (2011), Down syndrome and dementia: a randomized, controlled trial of antioxidant supplementation. Am J Med Genet A 155A:1939-1948

Martínez-Cué C, Martínez P, Rueda N, et al. (2013), Reducing GABAA α5 receptor-mediated inhibition rescues functional and neuromorphological deficits in a mouse model of down syndrome. J Neurosci 33:3953-3966.

Mele M, Leal G, Duarte CB (2016), Role of GABAA R trafficking in the plasticity of inhibitory synapses. J Neurochem 139:997-1018.

Nematullah M, Hoda MN, Khan F (2017), Protein Phosphatase 2A: a Double-Faced Phosphatase of Cellular System and Its Role in Neurodegenerative Disorders. Mol Neurobiol. 2017 Feb 21. doi: 10.1007/s12035-017-0444-3.

Parker SE, Mai CT, Canfield MA, Rickard R, Wang Y, Meyer RE, Anderson P, Mason CA, Collins JS, Kirby RS, Correa A (2010), National Birth Defects Prevention Network. (2010) Updated National Birth Prevalence estimates for selected birth defects in the United States, 2004-2006. Birth Defects Res A Clin Mol Teratol 88:1008-1016.

Pierobon M, Wulfkuhle J, Liotta L, Petricoin E. (2015) Application of molecular technologies for phosphoproteomic analysis of clinical samples. Oncogene. 34:805-14.

Pierobon M, Belluco C, Liotta LA, Petricoin EF 3rd. (2011) Reverse phase protein microarrays for clinical applications. Methods Mol Biol. 785:3-12.

Reeves R, Irving N, Moran T, Wohn A, Kitt C, Sisodia S, …., Davisson MT (1995), A mouse model for Down Syndrome exhibits learning and behaviour deficits. Nat genet 11:177-184.

Roubertoux PL, Carlier M (2010), Mouse models of cognitive disabilities in trisomy 21 (Down syndrome). Am J Med Genet C Semin Med Genet 154C:400-416.

Rueda N, Flórez J, Martínez-Cué C (2012), Mouse models of Down syndrome as a tool to unravel the causes of mental disabilities. Neural Plast 2012:584071.

Rueda N, Llorens-Martín M, Flórez J, Valdizán E, Banerjee P, Trejo JL, Martínez-Cué C (2010), Memantine normalizes several phenotypic features in the Ts65Dn mouse model of Down syndrome. J Alzheimers Dis 21:277-290.

Rueda N, Mostany R, Pazos A, Flórez J, Martínez-Cué C. (2005) Cell proliferation is reduced in the dentate gyrus of aged but not young Ts65Dn mice, a model of Down syndrome. Neurosci Lett. 380:197–201.

Schwanhäusser B, Busse D, Li N, Dittmar G, Schuchhardt J, Wolf J, Chen W, Selbach M (2011), Global quantification of mammalian gene expression control. Nature 473:337-342.

Serwanski DR, Miralles CP, Christie SB, Mehta AK, Li X, De Blas AL (2006), Synaptic and nonsynaptic localization of GABAA receptors containing the alpha5 subunit in the rat brain. J Comp Neurol 499:458-470.

Shichiri M, Yoshida Y, Ishida N, et al. (2011), α-Tocopherol suppresses lipid peroxidation and behavioral and cognitive impairments in the Ts65Dn mouse model of Down syndrome. Free Radic Biol Med 50:1801-1811.

Siarey RJ, Stoll J, Rapoport SI, Galdzicki Z (1997), Altered long-term potentiation in the young and old Ts65Dn mouse, a model for Down Syndrome. Neuropharmacology 36:1549-1554.

Silverman W (2007), Down syndrome: cognitive phenotype. Ment Retard Dev Disabil Res Rev 13: 228-236.

Song J, Zhong C, Bonaguidi MA, Sun GJ, Hsu D, Gu Y, Meletis K, Huang ZJ, Ge S, Enikolopov G, Deisseroth K, Luscher B, Christian KM, Ming GL, Song H. (2012) Neuronal circuitry mechanism regulating adult quiescent neural stem-cell fate decision. Nature. 489:150 –154.

Tozuka Y, Fukuda S, Namba T, Seki T, Hisatsune T. (2005) GABAergic excitation promotes neuronal differentiation in adult hippocampal progenitor cells. Neuron 47:803– 815.

Vogel C, Marcotte EM (2012), Insights into the regulation of protein abundance from proteomic and transcriptomic analyses. Nat Rev Genet 13:227-232.

Vilardell M, Rasche A, Thormann A, Maschke-Dutz E, Pérez-Jurado LA, Lehrach H, Herwig R (2011), Meta-analysis of heterogeneous Down Syndrome data reveals consistent genomewide dosage effects related to neurological processes. BMC Genomics 12: 229-239.

Table 1. Biological meaning of between-group comparisons

Comparison	Groups	MWM performance	
A	Ts65Dn-vehicle vs. control-vehicle	Failed vs. Normal	FvN
B	Ts65Dn-RO4938581 vs. Ts65Dn-vehicle	Rescued vs. Failed	RvF
C	Ts65Dn-RO4938581 vs. control-vehicle	Rescued vs. Normal	RvN
D	Control-RO4938581 vs. control-vehicle	Normal-RO4938581 vs. Normal	NRvN

MWM, Morris Water Maze. F, failed MWM performance; R, rescued MWM performance; N and NR (vehicle treated) and (RO4938581 treated) normal performance in the MWM.

Table 2. Numbers and magnitudes of protein differences between groups

	# protein differences			Magnitudes of differences (increases, decreases)			
	Total	Increased	Decreased	<20%	20%-30%	30%-50%	>50%
FvN	52	28	24	4,18	13,5	8,1	3,0
RvF	57	19	38	11,9	7,21	1,8	0,0
RvN	10	2	8	2,4	0,3	0,1	0,0
NRvN	13	9	4	9,2	0,2	0,0	0,0

Table 3. Expression differences in functional classes

	MAPK (19)	MTOR (15)	NMDAR (16)	AD-related (12)	IEG (4)	Apoptosis (5)
FvN	10	6	12	6	2	4
RvF	9	9	8	8	3	4
RvN	3	1	0	2	0	1
NRvN	5	3	4	1	0	0

Proteins within each class are listed in Appendix B (available from the authors). See also Figure 3 for NMDAR and related proteins.

Table 4. Signaling pathway perturbations (column 1) and responses after RO4938581 treatment (columns 2-4) in MAPK and MTOR pathway components.

	1	2	3	4
	FvN	RvF	RvN	NRvN
MAPK pathway				
BRAF	25%	-31%	-14%	-16%
ERK	37%	-24%		
pERK	20%	-37%	-24%	-23%
RSK	-16%	24%		17%
pRSK	37%	-36%		
PKCA	-10%	17%		
MTOR pathway				
AMPKA	35%	-33%		
AKT	47%	-27%		
pAKT		-25%	-27%	
pS6	42%	-37%		-20%
RAPTOR	17%	-17%		
GSK3B		-16%		
pGSK3BS9	-11%			
pGSK3BY212		13%		11%
pEIF4B	-18%	20%		11%

Table 5. Perturbations and responses to RO4938581 treatment of IEG, histone H3 modifications and a subset of AD-related proteins.

	FvN	RvF	RvN	NRvN		FvN	RvF	RvN	NRvN
IEGs					AD-related				
ARC					APP	59%	-29%	13%	
CFOS	-14%	20%			pTAU	26%	-26%		
pCFOS	18%	-22%			ERBB4		-14%	-17%	-26%
ERG1		-20%			pSRC	-16%	15%		
Histone modifications					CHAT	22%	-16%		
H3AcK18		-37%	-28%		IL1B	49%	-20%		
H3AcK9		-29%	-19%						

Table 6. Numbers of correlations for selected proteins.

Protein	V/R	Control	Common	Ts65Dn
NR1	V	0	3	9
	R	0,5	0,0	0,2
NR2A	V	2	6	10
	R	0	1,0	1,1
NR2B	V	1	4	9
	R	0,2	1,0	3,2
pNR1	V	2	5	12
	R	0	2	1,3
pNR2A	V	4	0	0
	R	0,1	1,1	5
pNR2B	V	0	4	14
	R	0,3	0	5,4
pGLUR2	V	1	3	16
	R	2,3	2,5	0,0
GLUR3	V	6	0	0
	R	1,8	0,6	0,0
GLUR4	V	3	0	0
	R	1,4	0,3	0,4
PP2A	V	4	4	18
	R	1,3	3,7 (C); 5,5 (T)	1
GAD2	V	1	0	1
	R	1,2	6,0	4,0
BDNF	V	1	0	8
	R	1,0	0,1	2,5
CFOS	V	2	2	16
	R	1,3	1,1	0,0
RSK	V	4	2	2
	R	1,3	1,8	1,1

V, vehicle treated; R, RO4938581 treated. In R, the # correlations seen in vehicle treated mice still present in drug treated mice and the # of new correlations are separated by commas.

Figure legends

Figure 1. RO4938581 improved Morris Water Maze performance in Ts65Dn mice. Data are presented as means ± S.E.M. of the latency to reach the platform during the twelve acquisition sessions by the four groups of mice. Data are pooled from Set 1 and Set 2 mice (data from Set 1 mice were from Martinez-Cue 2013). TS, Ts65Dn; CO, euploid controls. **: $p<0.01$; ***: $p<0.001$ TS vs. CO; #: $p<0.05$; ##: $p<0.01$ vehicle vs. RO4938581, Bonferroni post hoc tests after significant RM ANOVAS (ANOVA 'genotype': $F(1,39)=48.72$, $p<0.001$; 'treatment': $F(1,39)=0.17$, $p=0.17$; 'genotype x treatment': $F(1,39)=6.35$, $p=0.016$), i.e. there is a clear effect of genotype: Ts65Dn perform less well than euploid controls regardless of treatment.

Figure 2. Venn diagram showing the numbers of proteins that differed between genotypes and/or responded to drug treatment. A total of 91 proteins were measured; 23 proteins showed no change or difference in any comparison. Numbers within each circle and marked by arrows to each circle indicate the number of proteins of the total measured that changed or differed in each comparison. A. FvN, failed vs. normal learning/memory (LM): vehicle-treated Ts65Dn vs. vehicle-treated control. B. RvF, rescued vs. failed LM: RO4938581-treated Ts65Dn vs. vehicle-treated Ts65Dn. C. RvN, rescued vs. normal LM: RO4938581-treated Ts65Dn vs. vehicle-treated controls. D. NRvN, normal LM + RO4938581 vs. normal LM + vehicle. ↑, increased; ↓, decreased in comparison. Information in the box at the left could not be included without increasing the complexity of the Venn diagram. Changes/differences in 44 proteins are in opposite directions in comparisons A and B.

Figure 3. Magnitudes of differences and changes in levels of Hsa21 proteins (A-D) and NMDAR and related proteins (E-H) in each genotype/treatment group comparison. The % difference between groups is shown on the y-axis. The same proteins are presented in the same order in panels A-D and in panels E-H. Black bars, differences ≥10%, significant by 3-level mixed effects model with Benjamini-Hochberg correction for multiple testing, $p<0.05$, and FDR=5%. White bars, differences are not significant by the same criteria.

Figure 4. Examples of scatter plots from correlation analysis. Signal intensities for each of the 15 measurements (from 3 replicates of a 5 point dilution series) for each sample with each antibody

were normalized to the corresponding total protein levels and reduced to the mean for each sample. Selected pairs of proteins are shown with the Spearman Correlation values, r and p, in each graph. Criteria for significance: $r>|0.08|$, $p<0.05$. A-D, pNR1 vs. pNR2A in the 4 genotype-treatment groups: only the control + drug group fails to meet criteria for a significant correlation. E,F, GAD2 vs. PP2A in RO4938581 treated mice. G, DYRK1A vs. RCAN1 in control + vehicle mice: data cluster in two groups, mice with low values of both proteins and those with high values of both proteins. H, pNR2A vs. CFOS: data fail to show a monotonic relationship between the two proteins.

Figure 5. Networks of correlations involving NMDAR subunits. Pairwise correlations between protein levels were determined by Spearman correlation analysis; selected proteins with $r>|0.80|$ and $p<0.05$ are shown. Correlations present in A: vehicle-treated euploid and Ts65Dn; B: RO4938581-treated euploid mice; and C: RO4938581-treated Ts65Dn. Solid lines, correlations common to euploid and Ts65Dn mice. Dotted lines, correlations specific to euploid mice. Dashed lines, correlations specific to Ts65Dn. Shaded nodes, proteins involved in correlations common to euploid and Ts65Dn treated with vehicle.

Figure 6. Networks of correlations involving the protein phosphatase PP2A, regulatory subunit PPP2R1A. Pairwise correlations between protein levels were determined by Spearman correlation analysis; selected proteins with $r>|0.80|$ and $p<0.05$ are shown. Correlations present in A: vehicle-treated euploid and Ts65Dn, and B: RO4938581-treated euploid and Ts65Dn mice. Solid lines, correlations common to euploid and Ts65Dn mice. Dotted lines, correlations specific to euploid mice. Dashed lines, correlations specific to Ts65Dn. Shaded nodes, proteins present in vehicle and RO4938581 treated mice.

Figure 7. LTP pathway abnormalities in the Ts65Dn treated with vehicle (FvN) and treated with RO4938581 (RvN). The LTP pathway schematic was obtained from the Kyoto Encyclopedia of Genes and Genomes (KEGG) database; components and relationships between components are indicated by red rectangles and red arrows, respectively. Protein interactions with LTP pathway components were retrieved from the Human Protein Reference Database (HPRD), and the BioGRID and IntAct databases; interactors with evidence of expression in brain (Allen Brain

Atlas) were added to the pathway, as indicated by black ovals and black dotted lines. Proteins measured by RPPA are color coded: grey, no difference in FvN or RvN; yellow, different in FvN; green, different in RvN. For simplicity, a single node represents all forms measured of a single protein (both modification-independent and dependent). For magnitudes and directions of protein/protein modification differences specific to each node, see Appendix C.

Figure 8. Heat maps comparing protein abnormalities and responses to two drug treatment protocols. In each heatmap, lane 1: Ts65Dn vs. euploid controls (whole hippocampal lysates) after the behavioral battery and exposure to the MWM, plus vehicle or RO4938581; lanes 2 and 3: Ts65Dn vs. euploid controls (membrane, cytosol or nuclear subcellular fractions) after exposure to CFC (context-shock groups), plus saline or memantine (details are provided in Ahmed et al.. 2014, 2015). FvN: Ts65Dn failed LM vs. euploid control normal LM (vehicle or saline); RvN: Ts65Dn rescued LM (RO4938581 or memantine) vs. euploid control (vehicle or saline) normal LM. Separate heatmaps are shown to compare data obtained from whole hippocampal lysates with data obtained from subcellular fractions (A) cytosol and membrane and (B) cytosol and nuclear. (A) lane 1, whole hippocampal lysates; lanes 2 and 3, cytosol and membrane fractions, respectively. (B) lane 1, whole hippocampal lysates; lanes 2 and 3, nuclear and cytosol, respectively. Yellow, increased; blue, decreased; black, unchanged; grey, not measured or no expression detected.

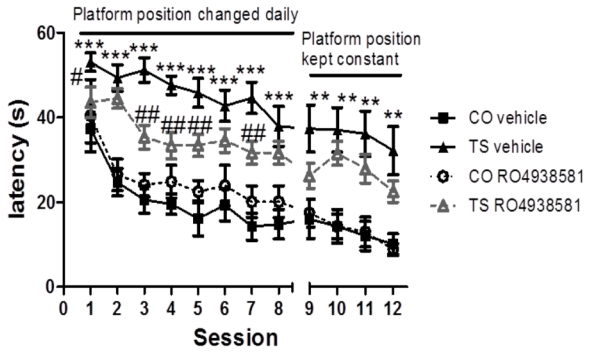

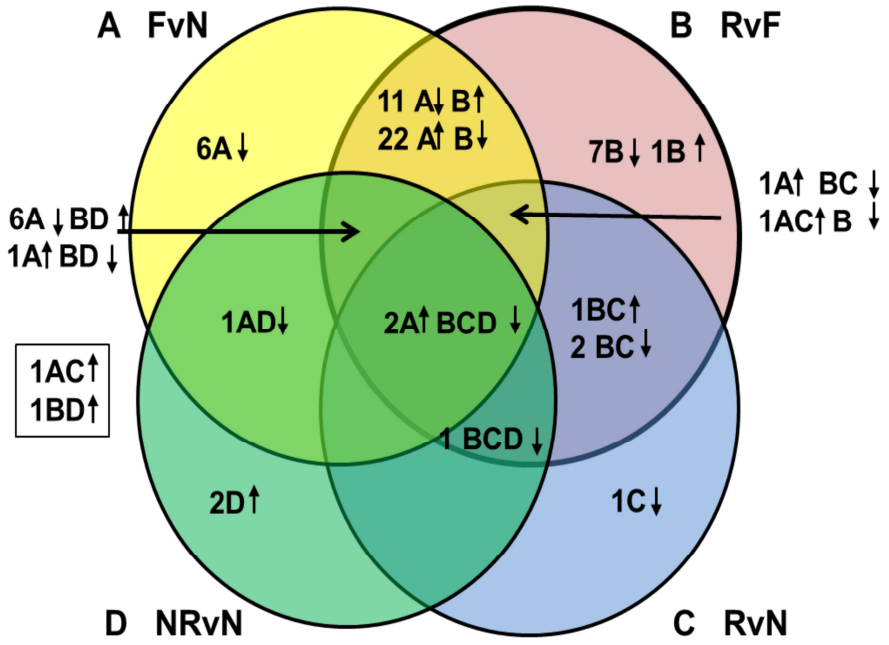

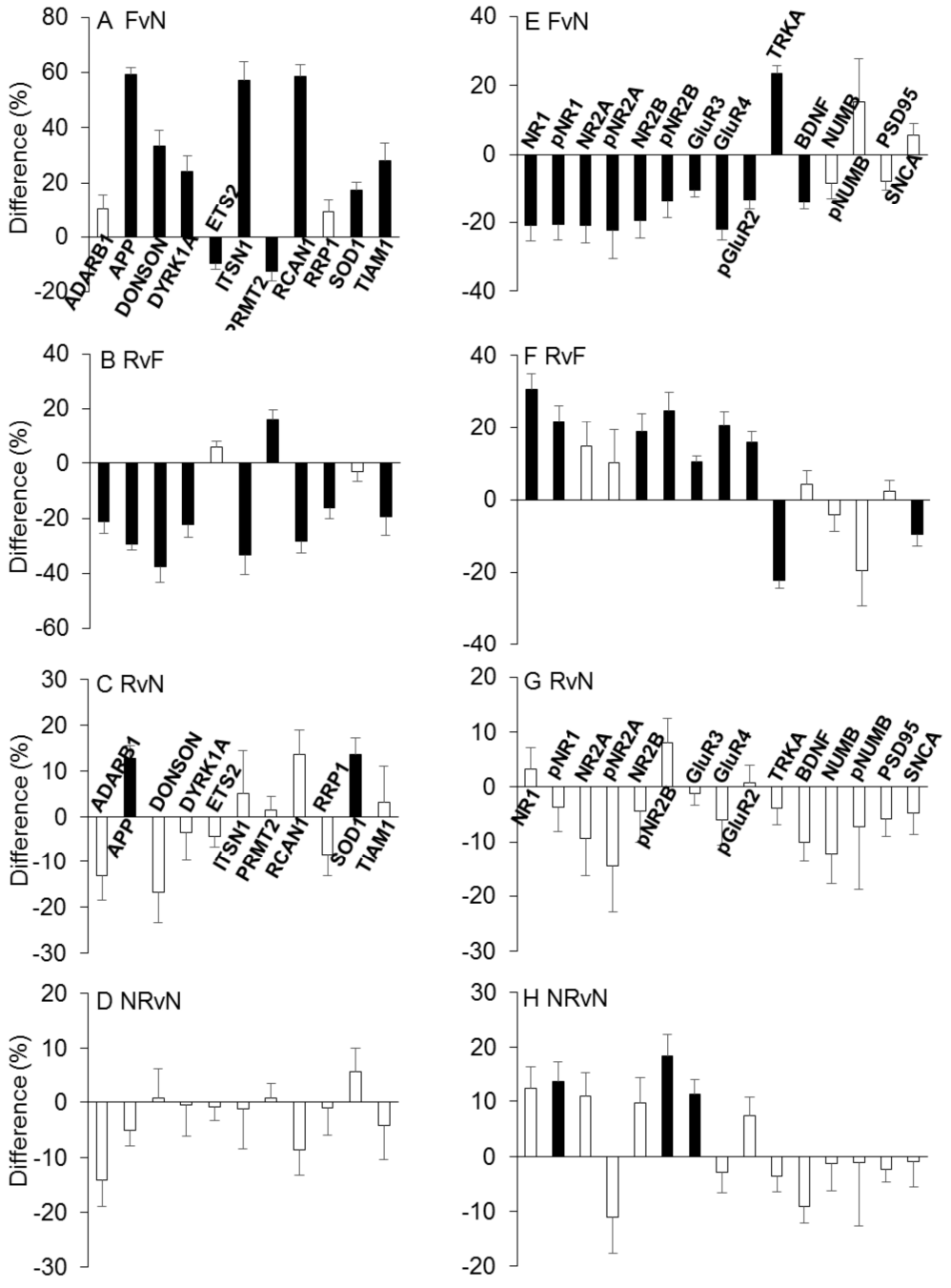
A FvN
Difference (%)
ADARB1
APP
DONSON
DYRK1A
ETS2
ITSN1
PRMT2
RCAN1
RRP1
SOD1
TIAM1
B RvF
C RvN
D NRvN
E FvN
NR1
pNR1
NR2A
pNR2A
NR2B
pNR2B
GluR3
GluR4
pGluR2
TRKA
BDNF
NUMB
pNUMB
PSD95
SNCA
F RvF
G RvN
H NRvN

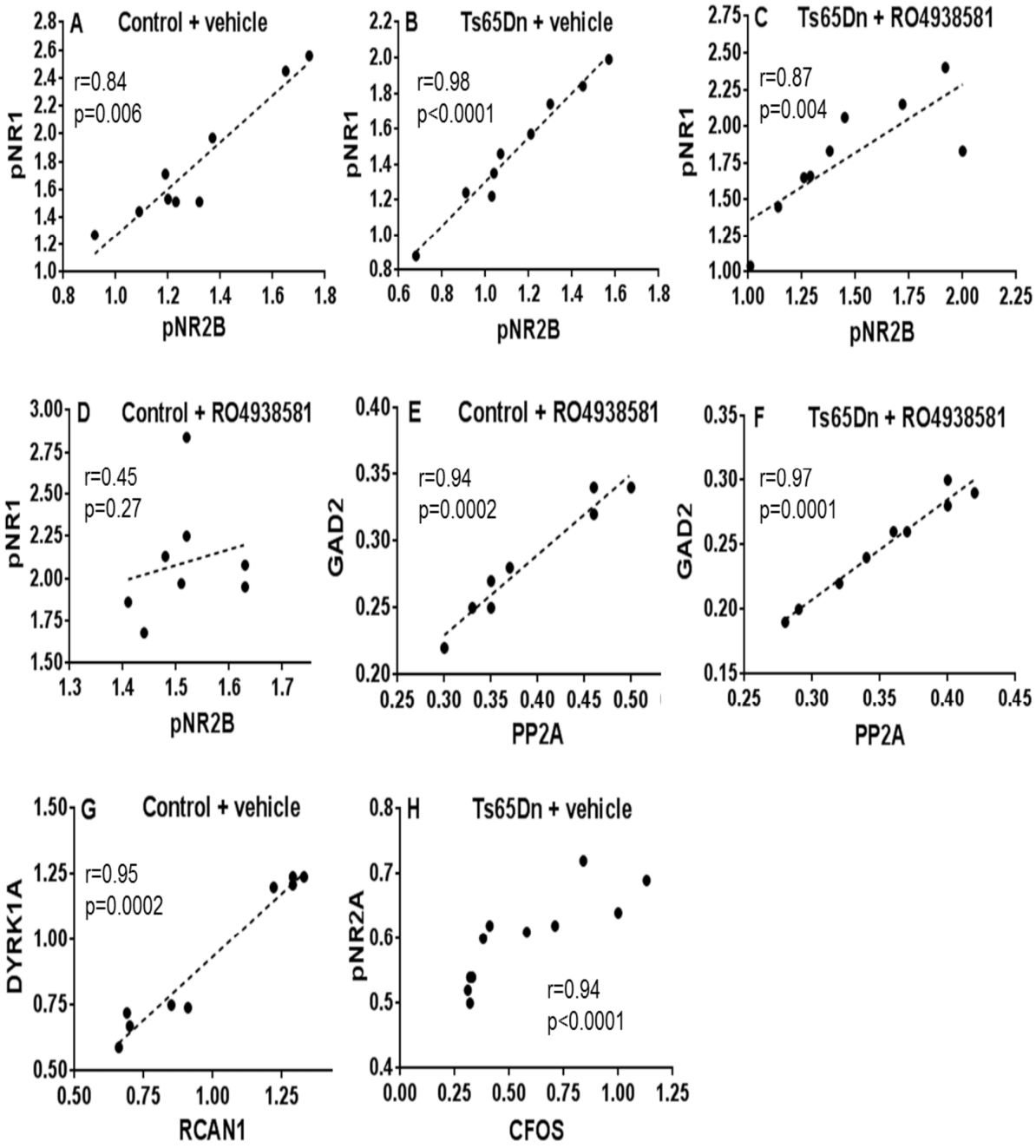
A
Control + vehicle
r=0.84
p=0.006
pNR1
pNR2B
B
Ts65Dn + vehicle
r=0.98
p<0.0001
pNR1
pNR2B
C
Ts65Dn + RO4938581
r=0.87
p=0.004
pNR1
pNR2B
D
Control + RO4938581
r=0.45
p=0.27
pNR1
pNR2B
E
Control + RO4938581
r=0.94
p=0.0002
GAD2
PP2A
F
Ts65Dn + RO4938581
r=0.97
p=0.0001
GAD2
PP2A
G
Control + vehicle
r=0.95
p=0.0002
DYRK1A
RCAN1
H
Ts65Dn + vehicle
r=0.94
p<0.0001
pNR2A
CFOS

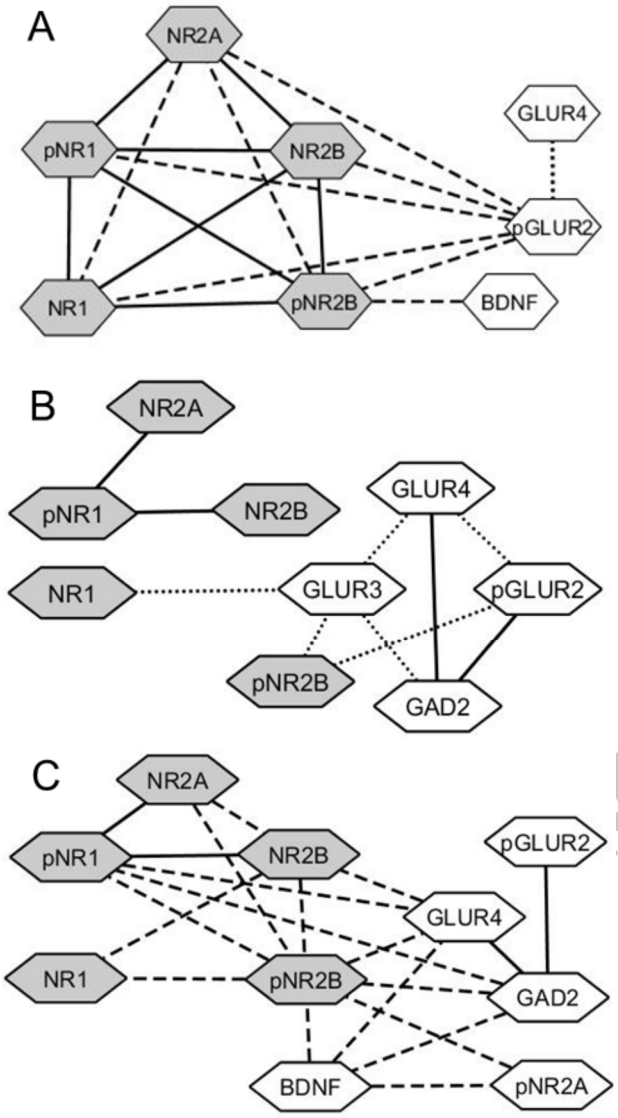

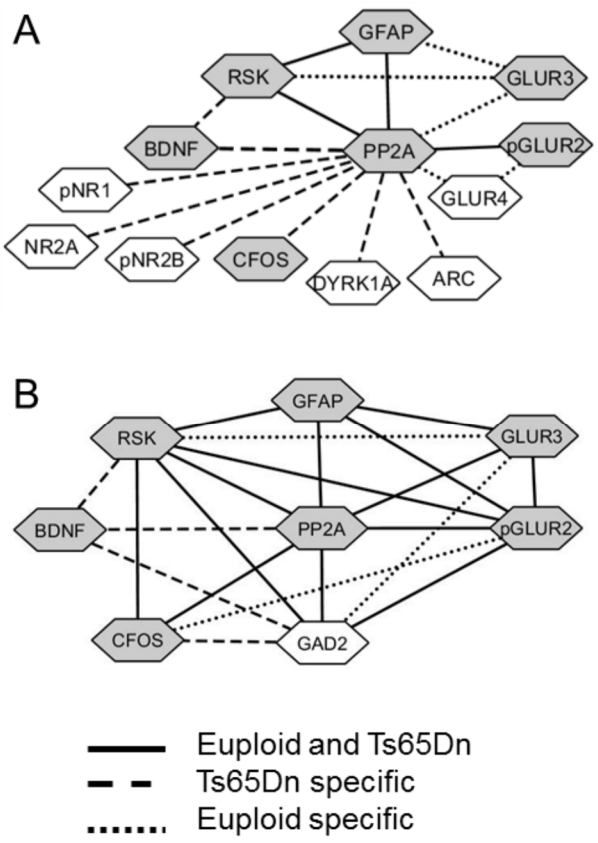

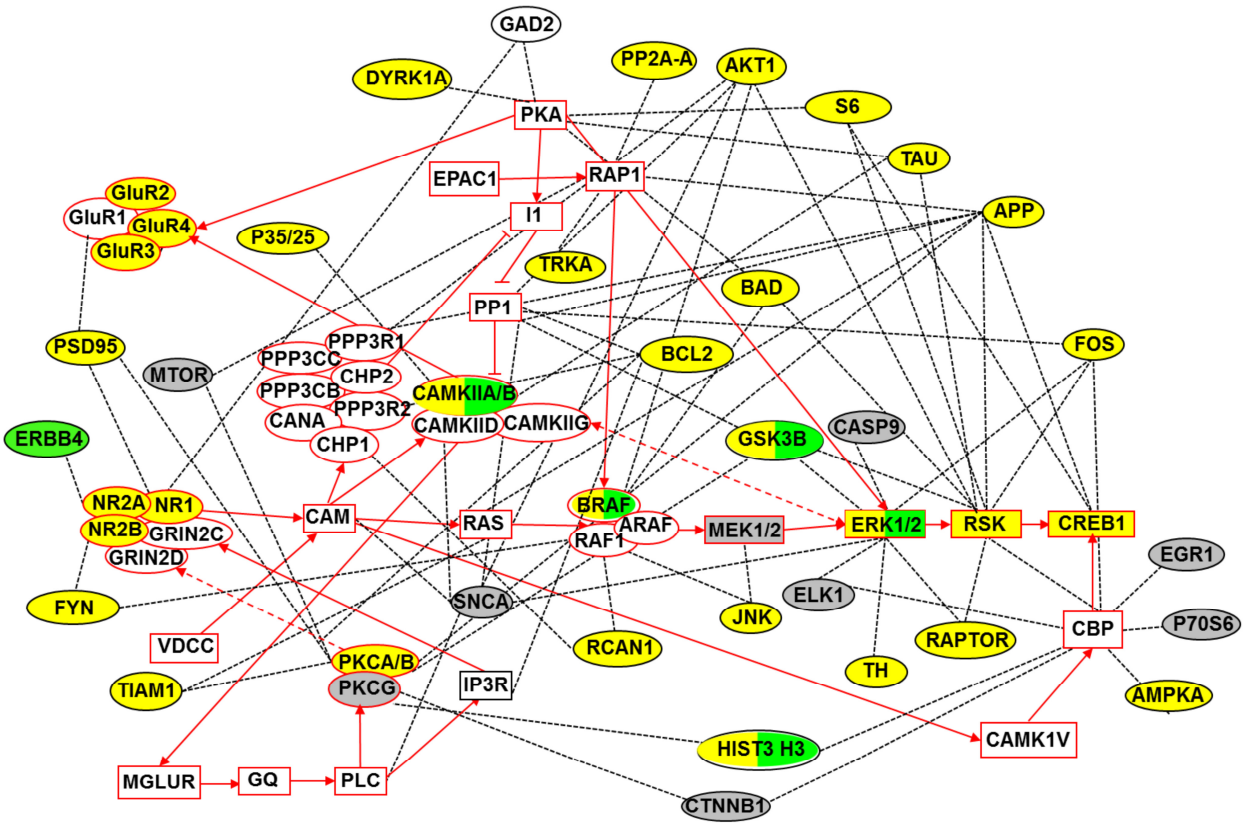

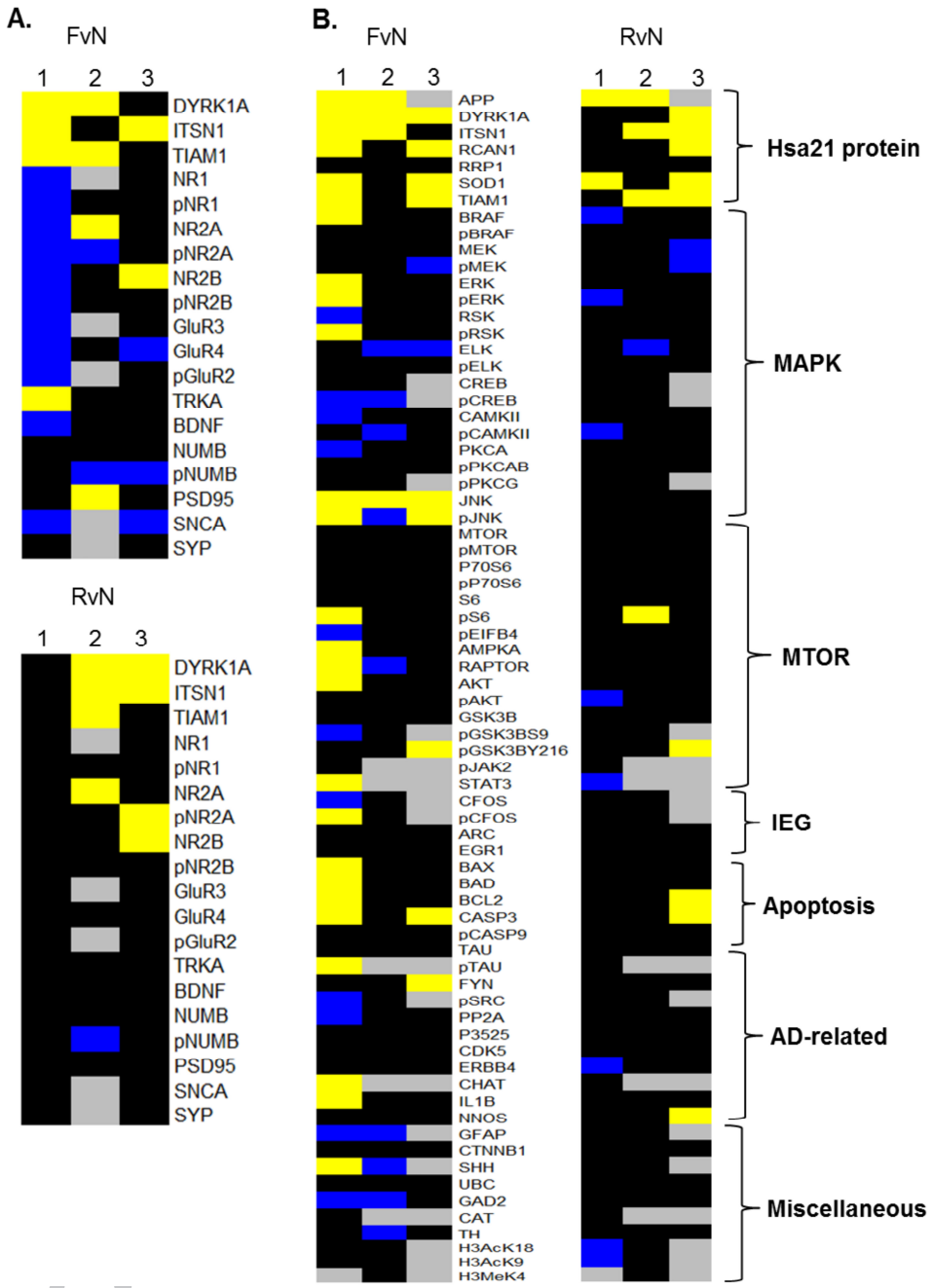

Appendix A. Information for individual mice. Mouse #, experimental animals; littermates, indicates animals housed together (not all littermates were experimental animals). Age, at sacrifice.

Set	Mouse #	Littermates	Age	Genotype	Treatment
1	97	98,99,100	6 months	Control	vehicle
1	101	102,103	6 months	Ts65Dn	vehicle
1	108	106,107	5 months and 3 weeks	Control	RO4938581
1	110	109,111	5 months and 3 weeks	Control	vehicle
1	111	109,110	5 months and 3 weeks	Control	vehicle
1	114	112,113	5 months and 3 weeks	Ts65Dn	vehicle
1	115	116	5 months and 3 weeks	Ts65Dn	vehicle
1	126	125,127,128	5 months and 2 weeks	Control	RO4938581
1	127	125,126,128	5 months and 2 weeks	Ts65Dn	RO4938581
1	149	148,150	6 months	Ts65Dn	RO4938581
1	151	152,153,154	6 months	Control	RO4938581
1	154	151,152,153	6 months	Ts65Dn	RO4938581
1	157	155,156	5 months and 3 weeks	Ts65Dn	RO4938581
1	158	159,160,161	5 months and 2 weeks	Control	RO4938581
1	162	163,164,165	5 months and 2 weeks	Control	RO4938581
1	180	181,182,183	5 months	Control	vehicle
1	187	188,189,190	5 months	Ts65Dn	vehicle
1	189	187,188,190	5 months	Ts65Dn	vehicle
1	191	192,193	5 months	Control	vehicle
2	725	727	6 months and 1 week	Ts65Dn	vehicle
2	728	729,730,731	6 months and 1 week	Control	vehicle
2	737	738,739	6 months	Ts65Dn	vehicle
2	738	737,739	6 months	Control	vehicle
2	740	741,742	6 months	Ts65Dn	RO4938581
2	741	740,742	6 months	Control	vehicle
2	742	740,741	6 months	Ts65Dn	RO4938581
2	747	746	5 months and 3 weeks	Control	RO4938581
2	748	751,752	5 months and 3 weeks	Ts65Dn	vehicle
2	753	754,755,756	5 months and 3 weeks	Control	vehicle

2	754	753,755,756	5 months and 3 weeks	Ts65Dn	vehicle
2	755	753,754,756	5 months and 3 weeks	Control	RO4938581
2	757	758,759,760	5 months and 2 weeks	Ts65Dn	RO4938581
2	758	757,759,760	5 months and 2 weeks	Ts65Dn	vehicle
2	759	757,758,760	5 months and 2 weeks	Control	vehicle
2	760	757,758,758	5 months and 2 weeks	Ts65Dn	RO4938581
2	761	762,763	5 months and 2 weeks	Control	RO4938581
2	763	761,762	5 months and 2 weeks	Control	vehicle
2	767	765,766,768	5 months and 1 week	Control	RO4938581
2	769	770,771,772	5 months	Ts65Dn	vehicle
2	771	769,770,772	5 months	Control	vehicle
2	772	769,770,771	5 months	Control	RO4938581
2	773	774,775,776	5 months	Ts65Dn	RO4938581
2	776	773,774,775	5 months	Ts65Dn	RO4938581

Appendix B. Protein and antibody information. All proteins are included, with common and official names and chromosome location (human/mouse). Functional class: ID, mutation in the human gene results in intellectual disability (Sturgeon et al 2012). LM, SP and ST: mutation of the mouse gene results in abnormal learning/memory, synaptic plasticity and synaptic transmission, respectively (information from the Mammalian Phenotype Browser, http://www.informatics.jax.org/searches/MP_form.shtml); Y, yes. Other: if not Hsa21: MAPK, protein is a component mitogen activated protein kinase pathawy; MTOR: protein is a component of the mechanistic target of rapamycin pathway; apoptosis, protein functions in apopotosis; IEG, immediate early gene; AD, reported abnormal in brains of patients with Alzheimer's Disease or mouse models of AD (see references in Table 1, Block et al 2014).

Common protein name	Official name		Functional class					Antibody Source	Catalogue #	Dilution
		chr	ID	LM	SP	ST	Other			
ADARB1	ADARB2	21/10				Y	HSA21	Aviva Systems Biology	ARP40342_T100	1:500
AKT	AKT1	14/12				Y	MTOR	Santa Cruz Biotechnology	SC-1619	1:300
AMPKA	PRKAA1	5/15					MTOR	Cell Signaling	2532	1:750
APP	APP	21/16		Y		Y	AD	Cell Signaling	2452	1:300
ARC	ARC	8/15		Y		Y	IEG	Abcam	Ab118929	1:300
BAD	BAD	11/19					Apoptosis	Cell Signaling	9292	1:500
BAX	BAX	19/7					Apoptosis	Cell Signaling	2772	1:750
BCL2	BCL2	18/1					Apoptosis	Cell Signaling	2870	1:500
BDNF	BDNF	11/2		Y	Y	Y	AD	Epitomics	2960-1	1:500
BRAF	BRAF	7/6	Y	Y		Y	MAPK	Cell Signaling	9434	1:500
CAMKII	CAMK2	5/18		Y	Y	Y	MAPK	Cell Signaling	3362	1:500
CaNA	PPP3CA	4/3					AD	Cell Signaling	2614	1:1000
Catalase	CAT	11/2					Oxidative stress	Abcam	Ab50434	1:500
CASP3	CASP3	4/8		Y	Y	Y	Apoptosis; AD	Cell Signaling	9662	1:500
CCT8	CCT8	21/16					HSA21	Aviva Systems Biology	ARP45837_P050	1:1000
CDK5	CDK5	7/5		Y		Y	AD	Cell Signaling	2506	1:500
cFOS	CFOS	14/12		Y		Y	IEG	Cell Signaling	2250	1:300
CHAF1B	CHAF1B	21/16					HSA21	Aviva Systems Biology	ARP45826_P050	1:750
CHAT	CHAT	10/14					AD	Millipore	AB1442	1:300
CREB	CREB1	2/1		Y		Y	MAPK	Cell Signaling	9197	1:500
DONSON	DONSON	21/16					HSA21	Aviva Systems Biology	ARP45862_P050	1:1000
DYRK1A	DYRK1A	21/16	Y				HSA21	Abnova	H00001859-M01	1:750
EGR1	EGR1	5/18		Y			IEG	Cell Signaling	4154	1:300
ERBB4	ERBB4	2/1		Y		Y	AD	Protein Technology	19943-1-AP	1:300
ERK1/2	MAPK1/3	22/16, 16/7		Y		Y	MAPK	Santa Cruz Biotechnology	SC-153	1:300
ETS2	ETS2	21/16					HSA21	Aviva Systems Biology	APR38592_P050	1:500
FTCD	FTCD	21/10	Y				HSA21	Aviva Systems Biology	APR41577_P050	1:1000

FYN	FYN	6/10		Y		Y	AD	Cell Signaling	4023	1:500
GAD2	GAD2	10/2						Cell Signaling	3988	1:1000
GFAP	GFAP	17/11	Y	Y		Y	AD	Epitomics	2301-1	1:500
GluR3	GRIA3	X/X	Y			Y	iGlut	Cell Signaling	5117	1:750
GluR4	GRIA4	11/9		Y		Y	iGlut	Cell Signaling	3824	1:300
GSK3B	GSK3B	3/16		Y		Y	MTOR; AD	BD Biosciences	610201	1:3000
HistoneH3 (AcK18)	HIST3H3	1/	Y				Histone modification	Cell Signaling	9675	1:300
HistoneH3 (AcK9)	HIST3H3	1/	Y				Histone modification	Cell Signaling	9649	1:300
HistoneH3 (DMeK4)	HIST3H3	1/	Y				Histone modification	Cell Signaling	9725	1:300
IL1B	IL1B	2/2					AD	Abnova	H00003553	1:3000
ITSN1	ITSN1	21/16					HSA21	BD Biosciences	611574	1:1500
JNK	MAPK8	10/14					MAPK	Cell Signaling	9252	1:500
MEK1/2	MAP2K1/2	15/9, 19/10	Y				MAPK	Cell Signaling	9122	1:500
MTOR	MTOR	1/4					MTOR	Cell Signaling	2972	1:500
nNOS	NOS1	12/5		Y		Y	AD	Cell Signaling	4234	1:500
NR1	GRIN1	9/2	Y	Y	Y	Y	AD; iGlut	Upstate Biotechnology	07-362	1:500
NR2A	GRIN2A	16/16	Y	Y		Y	AD; iGlut	PhosphoSolutions	1497-NR2A	1:500
NR2B	GRIN2B	12/6	Y	Y	Y	Y	AD;iGlut	PhosphoSolutions	1498-NR2B	1:500
NUMB	NUMB	14/12					AD	Cell Signaling	2756	1:500
P35/25	CDK5R1	17/11		Y		Y	AD	Cell Signaling	2680	1:750
P38	MAPK14	6/17					MAPK	Cell Signaling	9212	1:500
P70S6	RPS6KB1	17/11					MTOR	Santa Cruz Biotechnology	SC-8418	1:400
pAKT (Ser473)	AKT1	14/12				Y	MTOR	Cell Signaling	4060	1:500
pBRAF(Thr401)	BRAF	7/6	Y	Y		Y	MAPK	Epitomics	2298-1	1:1000
pCAMKIIA/B□□□ Thr286)	CAMK2A/B	5/18		Y	Y	Y	MAPK	PhosphoSolutions	p1005-286	1:4000
pCASP9(Ser196)	CAPS9	1/4					Apoptosis	Abgent	AP3044a	1:300
pcFOS	CFOS	14/12		Y		Y	IEG	Cell Signaling	5348	1:300
pCREB(Ser133)	CREB1	2/1		Y		Y	MAPK	PhosphoSolutions	p1010-133	1:500
pEIF4B(Ser422)	EIF4B	12/15					MTOR	Cell Signaling	3591	1:500
pELK1 (Ser383)	ELK1	X/X					MAPK	Santa Cruz Biotechnology	SC-8406	1:500
pERK1/2(Tyr204)	MAPK1/3	22/16, 16/7		Y		Y	MAPK	Santa Cruz Biotechnology	SC-7383	1:500
pGJA1 (Ser368)		6/10						Abnova	PAB9652	1:500

pGluR2(Tyr876)	GRIA2	4/3		Y	Y	Y	iGlut	Cell Signaling	4027	1:500
pGSK3B(Ser9)	GSK3B	3/16		Y		Y	MTOR; AD	Cell Signaling	9323	1:750
pGSK3B□(Tyr216)	GSK3B	3/16		Y		Y	MTOR; AD	BD Biosciences	612312	1:2000
PI3K	PIK3CA	3/3					MTOR	Cell Signaling	4249	1:500
pJNK(Thr183/Tyr185)	MAPK8	10/14					MAPK	Cell Signaling	9251	1:1000
PKCA	PRKCA	17/11					MAPK	Cell Signaling	2056	1:500
pMEK1/2(Ser217/221)	MAP2K1/2	15/9, 19/10	Y				MAPK	Cell Signaling	9154	1:750
pMTOR(Ser2448)	MTOR	1/4					MTOR	Cell Signaling	2971	1:500
pNR1(Ser889)	GRIN1	9/2	Y	Y	Y	Y	AD; iGlut	Epitomics	2329-1	1:500
pNR2A(Tyr1246)	GRIN2A	16/16	Y	Y		Y	AD; iGlut	Cell Signaling	4206	1:500
pNR2B(Tyr1336)	GRIN2B	12/6	Y	Y	Y	Y	AD; iGlut	PhosphoSolutions	p1516-1336	1:500
pNUMB(Ser276)	NUMB	14/12					AD	Cell Signaling	4140	1:500
PP2A	PPP2R1A	19/17					AD	Cell Signaling	2041	1:750
pP70S6(Thr389)	RPS6KB1	17/11					MTOR	Cell Signaling	9205	1:500
pPKCA/B(Thr638/641)	PRKAA/B	17/11					MAPK	Cell Signaling	9375	1:750
pPKCG (Thr514)	PRKCAG	17/11	Y	Y		Y	MAPK	Cell Signaling	9379	1:750
PRMT2	PRMT3	21/10					HSA21	Aviva Systems Biology	ARP40196_T100	1:2000
pRSK(Ser380)	RPS6KA3	X/X	Y				MAPK	Cell Signaling	9341	1:500
pS6(Ser240/244)	RPS6	9/4					MTOR	Cell Signaling	5364	1:500
PSD95	DLG4	17/11		Y		Y	AD	Cell Signaling	3450	1:1000
pSRC(Tyr416)	FYN	6/10		Y		Y	AD	Cell Signaling	6943	1:500
pTau (Thr212)	MAPT	17/11		Y		Y	AD	Invitrogen	44740G	1:3000
RAPTOR	RPTOR	17/11					MTOR	Cell Signaling	2280	1:750
RCAN1	RCAN1	21/16					HSA21	Sigma-Aldrich	D6694	1:2000
RRP1	RRP1	21/10					HSA21	Aviva Systems Biology	ARP45812_P050	1:2000
RSK2	RPS6KA3	X/X	Y				MAPK	Cell Signaling	9340	1:300
S6	RPS6	9/4					MTOR	Cell Signaling	2217	1:500
SHH	SHH	7/5	Y				Sonic Hedgehog	Cell Signaling	2207	1:500
SOD1	SOD1	21/16					HSA21	Santa Cruz Biotechnology	SC-11407	1:500
STAT3	STAT3	17/11					JAK-STAT	Cell Signaling	9139	1:500
SYP	SYP	X/X	Y				AD	Epitomics	1870-1	1:5000
Tau	MAPT	17/11		Y		Y	AD	Cell Signaling	4019	1:500
TH	TH	11/7	Y	Y			AD	Cell Signaling	2792	1:750
TIAM1	TIAM1	21/16					HSA21	Abcam	Ab54458	1:1500

TRKA	NTRK1	1/3	Y	Y			AD	Epitomics	2244-1	1:2000
Ubiquitin	UBC	12/5					Ubiquitination	Cell Signaling	3933	1:1000
□□Synuclein	SNCA	4/6				Y	AD	Cell Signaling	4179	1:3000
□-Catenin	CTNNB1	3/9	Y				AD	Cell Signaling	9562	1:1000

Appendix C

3-level mixed effects results protein measurements

3LME results

Protein	VehicleTs65Dr	PValue	Error	StepdownB	AdaptiveH	FDR	Protein	Control RO493	PValue	Error	StepdownB	AdaptiveH	FDR
ADARB1	1.04E+01	6.28E-02	5.27E+00	1.00E+00	5.66E-01	8.17E-02	ADARB1	-1.41E+01	1.98E-03	4.80E+00	1.46E-01	9.70E-02	9.36E-03
AKT	4.73E+01	6.34E-11	5.63E+00	4.82E-09	5.71E-10	3.61E-10	AKT	6.30E+00	2.69E-01	5.51E+00	1.00E+00	9.63E-01	4.37E-01
AMPKA	3.46E+01	4.82E-14	3.65E+00	4.00E-12	4.34E-13	4.46E-13	AMPKA	-4.49E+00	2.66E-01	4.12E+00	1.00E+00	9.63E-01	4.37E-01
APP	5.93E+01	2.62E-44	2.56E+00	2.39E-42	2.36E-43	2.39E-42	APP	-5.06E+00	8.09E-02	2.96E+00	1.00E+00	9.63E-01	1.71E-01
ARC	2.69E+00	6.16E-01	5.28E+00	1.00E+00	9.87E-01	6.37E-01	ARC	-1.27E+01	3.72E-03	4.61E+00	2.57E-01	1.82E-01	1.47E-02
BAD	3.26E+01	6.48E-18	2.95E+00	5.77E-16	5.83E-17	1.97E-16	BAD	-1.60E+00	7.01E-01	4.20E+00	1.00E+00	9.63E-01	8.62E-01
BAX	2.53E+01	2.26E-17	2.45E+00	1.99E-15	2.03E-16	5.14E-16	BAX	-7.51E+00	5.85E-03	2.80E+00	3.86E-01	2.87E-01	2.05E-02
BCL2	2.13E+01	1.83E-09	3.05E+00	1.32E-07	1.65E-08	8.34E-09	BCL2	-7.07E+00	8.98E-02	4.30E+00	1.00E+00	9.63E-01	1.82E-01
BDNF	-1.37E+01	1.85E-08	2.50E+00	1.31E-06	1.66E-07	8.00E-08	BDNF	-9.16E+00	1.76E-03	3.02E+00	1.32E-01	8.60E-02	9.36E-03
BRAF	2.52E+01	3.15E-12	3.04E+00	2.49E-10	2.83E-11	2.20E-11	BRAF	-1.56E+01	1.17E-06	3.37E+00	1.04E-04	5.71E-05	3.53E-05
CAMKII	-1.07E+01	6.60E-04	3.26E+00	2.77E-02	5.94E-03	1.20E-03	CAMKII	1.60E+01	3.19E-06	3.08E+00	2.80E-04	1.56E-04	7.25E-05
CASP3	2.34E+01	1.76E-11	2.91E+00	1.38E-09	1.59E-10	1.15E-10	CASP3	-1.06E+01	2.84E-03	3.70E+00	1.99E-01	1.39E-01	1.17E-02
CAT	-7.54E+00	2.08E-02	3.37E+00	6.23E-01	1.87E-01	3.05E-02	CAT	1.25E+01	1.89E-05	2.68E+00	1.62E-03	9.26E-04	2.87E-04
CDK5	-1.39E+01	1.70E-02	6.23E+00	5.45E-01	1.53E-01	2.58E-02	CDK5	-1.55E+01	2.12E-03	5.43E+00	1.53E-01	1.04E-01	9.36E-03
CFOS	-1.35E+01	4.67E-10	2.23E+00	3.41E-08	4.20E-09	2.23E-09	CFOS	6.65E+00	7.70E-04	1.89E+00	6.08E-02	3.77E-02	5.39E-03
CHAT	2.19E+01	2.36E-13	2.53E+00	1.89E-11	2.12E-12	1.79E-12	CHAT	2.12E+00	5.18E-01	3.24E+00	1.00E+00	9.63E-01	6.64E-01
CREB	-9.32E+00	4.65E-05	2.35E+00	2.37E-03	4.18E-04	1.03E-04	CREB	1.14E+01	2.14E-04	2.87E+00	1.71E-02	1.05E-02	1.62E-03
CTNNB1	-1.04E+01	3.16E-02	5.09E+00	8.53E-01	2.84E-01	4.42E-02	CTNNB1	2.37E+00	6.21E-01	4.74E+00	1.00E+00	9.63E-01	7.85E-01
DONSON	3.34E+01	1.09E-06	5.68E+00	6.40E-05	9.77E-06	2.99E-06	DONSON	7.19E-01	8.96E-01	5.49E+00	1.00E+00	9.63E-01	9.27E-01
DYRK1A	2.42E+01	1.28E-04	5.52E+00	6.27E-03	1.15E-03	2.71E-04	DYRK1A	-4.45E-01	9.38E-01	5.72E+00	1.00E+00	9.63E-01	9.48E-01
EGR1	1.54E+01	4.29E-02	7.03E+00	1.00E+00	3.86E-01	5.91E-02	EGR1	-1.42E+01	9.07E-03	5.79E+00	5.89E-01	4.44E-01	3.06E-02
ELK	-4.21E+00	1.93E-01	3.30E+00	1.00E+00	9.87E-01	2.31E-01	ELK	-8.70E-01	7.89E-01	3.27E+00	1.00E+00	9.63E-01	8.87E-01
ERBB4	-3.47E+00	4.37E-01	4.54E+00	1.00E+00	9.87E-01	4.79E-01	ERBB4	-2.59E+01	9.23E-13	3.81E+00	8.40E-11	4.52E-11	8.40E-11
ERK	3.65E+01	5.84E-08	5.43E+00	3.91E-06	5.25E-07	2.12E-07	ERK	-6.20E+00	3.45E-01	6.75E+00	1.00E+00	9.63E-01	5.27E-01
ETS2	-9.82E+00	1.34E-06	2.08E+00	7.64E-05	1.21E-05	3.48E-06	ETS2	-8.15E-01	7.40E-01	2.46E+00	1.00E+00	9.63E-01	8.74E-01
FYN	-7.62E+00	2.78E-01	7.29E+00	1.00E+00	9.87E-01	3.20E-01	FYN	1.71E+00	8.09E-01	7.01E+00	1.00E+00	9.63E-01	8.98E-01
GAD2	-1.14E+01	2.53E-08	2.09E+00	1.74E-06	2.28E-07	1.00E-07	GAD2	5.53E+00	5.78E-02	2.82E+00	1.00E+00	9.63E-01	1.31E-01
GFAP	-1.12E+01	6.32E-06	2.56E+00	3.41E-04	5.68E-05	1.51E-05	GFAP	1.05E+01	2.16E-03	3.22E+00	1.53E-01	1.06E-01	9.36E-03
GluR3	-1.04E+01	3.31E-08	1.91E+00	2.25E-06	2.98E-07	1.25E-07	GluR3	1.13E+01	4.17E-05	2.57E+00	3.42E-03	2.04E-03	3.80E-04
GluR4	-2.20E+01	1.51E-13	3.14E+00	1.22E-11	1.36E-12	1.25E-12	GluR4	-2.87E+00	4.44E-01	3.80E+00	1.00E+00	9.63E-01	6.03E-01
GSK3B	-4.57E+00	8.96E-02	2.74E+00	1.00E+00	8.07E-01	1.15E-01	GSK3B	1.84E+00	5.02E-01	2.71E+00	1.00E+00	9.63E-01	6.53E-01
H3K18	-1.97E+01	1.39E-04	5.62E+00	6.69E-03	1.25E-03	2.88E-04	H3K18	-5.81E+00	2.58E-01	5.28E+00	1.00E+00	9.63E-01	4.37E-01
H3K27	1.38E+01	1.26E-02	5.11E+00	4.14E-01	1.13E-01	1.94E-02	H3K27	-4.55E+00	3.59E-01	5.06E+00	1.00E+00	9.63E-01	5.36E-01
IL1B	4.89E+01	2.49E-08	6.78E+00	1.74E-06	2.24E-07	1.00E-07	IL1B	1.09E+01	8.87E-02	6.05E+00	1.00E+00	9.63E-01	1.82E-01
ITSN1	5.71E+01	2.61E-10	6.78E+00	1.96E-08	2.35E-09	1.40E-09	ITSN1	-1.21E+00	8.67E-01	7.29E+00	1.00E+00	9.63E-01	9.27E-01
JNK	2.87E+01	7.04E-17	2.77E+00	6.05E-15	6.34E-16	1.07E-15	JNK	-9.35E+00	1.05E-03	2.95E+00	8.23E-02	5.17E-02	6.46E-03
MEK	-5.48E-02	9.87E-01	3.37E+00	1.00E+00	9.87E-01	9.87E-01	MEK	-9.45E-01	7.49E-01	2.97E+00	1.00E+00	9.63E-01	8.74E-01
MTOR	1.01E+01	2.31E-02	4.18E+00	6.70E-01	2.08E-01	3.34E-02	MTOR	-5.25E+00	2.64E-01	4.81E+00	1.00E+00	9.63E-01	4.37E-01
NNOS	-8.24E+00	3.14E-01	8.51E+00	1.00E+00	9.87E-01	3.53E-01	NNOS	-8.82E+00	2.04E-01	7.23E+00	1.00E+00	9.63E-01	3.62E-01
NR1	-2.10E+01	5.72E-07	4.57E+00	3.49E-05	5.15E-06	1.68E-06	NR1	1.24E+01	4.29E-03	4.06E+00	2.92E-01	2.10E-01	1.63E-02
NR2A	-2.10E+01	5.95E-06	5.08E+00	3.27E-04	5.36E-05	1.46E-05	NR2A	1.10E+01	2.14E-02	4.49E+00	1.00E+00	9.63E-01	6.10E-02
NR2B	-1.95E+01	1.97E-05	4.98E+00	1.02E-03	1.77E-04	4.48E-05	NR2B	9.77E+00	3.98E-02	4.50E+00	1.00E+00	9.63E-01	9.79E-02
NUMB	-8.40E+00	5.93E-02	4.63E+00	1.00E+00	5.34E-01	7.82E-02	NUMB	-1.35E+00	7.82E-01	4.91E+00	1.00E+00	9.63E-01	8.87E-01
P3525	-8.45E+00	2.04E-03	2.83E+00	8.36E-02	1.84E-02	3.64E-03	P3525	-3.83E+00	1.89E-01	2.96E+00	1.00E+00	9.63E-01	3.44E-01

Highlights

- Levels of 91 proteins relevant to brain function were measured in Ts65Dn hippocampus after training in the Morris Water Maze
- Levels of 55 proteins/protein modifications were abnormal in vehicle-treated Ts65Dn compared with littermate controls
- the GABAAα5-selective modulator, RO4938581, that rescues learning deficits, corrected the majority of protein abnormalities
- protein abnormalities, and their correction, are consistent with abnormalities in and rescue of LTP